UNIVERSIDADE DE LISBOA
FACULDADE DE CIÊNCIAS
DEPARTAMENTO DE BIOLOGIA ANIMAL

Helicobacter hepaticus colonization in mice: newborn tolerance properties and distribution throughout the gut

Mestrado em Biologia Evolutiva e do Desenvolvimento

Margarida Araújo

Dissertação orientada por:
Professor Doutor Élio Sucena (IGC, FCUL)
Doutora Jocelyne Demengeot (IGC)

2014/2015

AGRADECIMENTOS

Em primeiro lugar, quero agradecer à Doutora Jocelyne Demengeot por me ter recebido no seu grupo de investigação no Instituto Gulbenkian de Ciência. Pela oportunidade que me deu para desenvolver o meu projeto de Mestrado no seu grupo, pela sua orientação durante todo o seu processo de desenvolvimento, tanto na fase inicial em que foi delineado como no decorrer do mesmo ao longo do ano, pela confiança que depositou em mim e no meu trabalho, pela sua disponibilidade, e pelo seu feedback acerca dos resultados que foram sendo apresentados.

Em segundo lugar, agradeço ao Rômulo Areal pelo seu empenho na minha supervisão, pela sua constante orientação desde o primeiro dia em que cheguei ao laboratório, pelo conhecimento que me transmitiu em grande parte das técnicas experimentais e análise de resultados mencionados neste trabalho pressupondo uma enorme paciência da sua parte, pelo sentido de organização e método que me passou ao longo do ano aplicado às diversas experiências e pelo seu acompanhamento sempre que necessário, pela sua acessibilidade e, acima de tudo, pelo seu apoio mesmo após ter conhecimento de que algo não correu como previsto.

Agradeço à Catarina Nunes, colega de Mestrado, pela sua enorme amizade e companheirismo para comigo, por todos os momentos de desabafo, pela companhia ao almoço, ao lanche e nos seminários.

Agradeço também à Ana Regalado, pelo bom ambiente que criou ao longo do ano, quase todos os dias, no nosso laboratório, por me perguntar sempre como estava o meu cão e por todos os chocolates que me ofereceu.

Por ordem cronológica, e não de importância:

À Joana Silva, pela ajuda que me deu a perceber vários protocolos, como o de extração de DNA de gel de agarose, transformação de bactérias para clonagem molecular e pela sua prontidão na resposta a todos os emails que lhe foram enviados.

À Vânia Silva, quando precisei de recolher amostras de sangue dos animais.

Ao José Santos, pelas dúvidas que iam surgindo momentaneamente e que foram sempre retiradas.

À Lisa Bergman, pela sua ajuda na tentativa de reproduzir a deteção de duas populações dentro da população de bactérias fecais IgA^+ em animais colonizados em adulto com *Hh* que haviam sido detetadas anteriormente com o

objetivo de sorting e subsequente análise por sequenciação da região 16S do rRNA dos grupos bacterianos presentes em cada uma delas.

Ao Vasco Correia e à Íris Caramalho, que foram recebidos posteriormente no nosso grupo mas que revelaram sempre uma grande prontidão e disponibilidade para me ajudar.

Não posso deixar de agradecer especialmente à Inês Cabral, pela sua boa disposição no laboratório e, principalmente, pelo facto de ter ficado com a responsabilidade de tratar da nossa colónia de animais durante os últimos dois meses.

A todos os funcionários da Animal House do Instituto Gulbenkian de Ciência:

À Joana Bom pela sua disponibilidade em atender os meus pedidos de animais mesmo não sendo cumprido o tempo de antecedência necessário e às minhas dúvidas relativamente à cultura de amostras dos nossos animais submetidos a mono-colonização em meio TB para confirmar o seu estado de colonização única com *Helicobacter*.

À Ana Lúcia Ribeiro, pela sua ajuda na Gnotobiology room onde foram mantidos os animais germ-free, pela sua disponibilidade, o que envolveu a perda de muitas manhãs do seu trabalho e alguma paciência dado todos os procedimentos necessários para que uma instalação germ-free mantenha essa definição.

Ao Manuel Rebelo, pela sua prontidão em resolver os problemas eletrónicos com a porta de acesso à sala onde foram mantidos os animais colonizados com *Helicobacter*.

Ao Lévi Pires, pelos pedidos de material necessário para a sala dos animais colonizados com *Helicobacter*.

RESUMO

Diferentes estudos desenvolvidos pelo nosso grupo envolveram colonização com *Helicobacter hepaticus* (*Hh*) reproduzindo um tipo de interação hospedeiro-microorganismo. Dados anteriores aos que são apresentados neste projeto reportaram que após a colonização com *Hh* em ratos adultos saudáveis B6 WT é desencadeada uma resposta robusta de imunoglobulina (Ig) específica contra *Hh*, acompanhada por uma redução da densidade bacteriana (dados não pulicados). Também foi observado que é necessária uma resposta de células B dependente de células T para controlar a densidade de *Hh* e que a citoquina responsável pela persistência de *Hh*, IL-10, é essencial para modular esta resposta. Curiosamente, aquando da colonização com esta bactéria em ratos neonatos B6 WT, a resposta de Igs específicas não se verificou e estes animais apresentaram densidades elevadas de *Hh*. Por fim, a tolerância a *Hh* – mediada por IL-10 e sustentada por células T regulatórias $CD25^+$ – foi mantida mesmo quando os animais atingiram a idade adulta (dados não publicados).

Tendo em conta as evidências referidas acima, o grande foco deste trabalho residiu no contraste entre a colonização com *Hh* no período neonatal e no adulto. Neste contexto, decidimos explorar o papel da presença de uma microbiota complexa na resposta de tolerância a *Hh*. Assim, a partir de animais GF (desprovidos de qualquer microorganismo) B6 foram produzidos animais Ad.mcol – colonização ig com *Hh* de cultura em ratos com 8 semanas e analisados 9 semanas pós-colonização – e animais Nb.mcol – nascidos a partir de mães mono-colonizadas com *Hh* e analisados com 9 semanas de idade. Semelhante ao que tinha sido demonstrado para animais SPF Nb.col (dados não publicados), não foi detetada IgA anti-*Hh* nas fezes de ratos Nb.mcol provando que a tolerância a *Hh* é independente da microbiota.

Para além disso, demonstrámos que a Ig específica contra *Hh* se liga diretamente à sua superfície. Isto foi inferido através da incubação de extratos fecais de ratos Ad.col e Nb.col, usando como controlo negativo animais SPF, com *Hh* crescida em cultura. Posteriormente, a análise por citometria de fluxo confirmou que o anticorpo produzido especificamente contra *Hh* se liga efetivamente à sua superfície, o que ainda não tinha sido demonstrado até ao momento. A concentração de IgA detetada através de ELISA envolve a incubação de amostras de fezes com um lisado de *Hh,* sendo apenas determinada a IgA específica que a reconhece e se liga aos seus antigénios. Pelo contrário, uma vez que incubámos amostras de fezes com uma suspensão de *Hh* crescida em cultura no ensaio descrito acima, a integridade estrutural da parede celular bacteriana não foi comprometida. Assim, foi possível replicar a interação entre o sistema imunitário do hospedeiro e as bactérias num contexto *in vivo*, sendo considerado como um modelo plausível do que acontece ao nível fisiológico quando a IgA encontra estas bactérias

intactas dentro do hospedeiro: a IgA reconhece os antigénios que se encontram na superfície de *Hh* presente no lúmen do intestino e a sua afinidade promove uma ligação específica; estes microorganismos ficam revestidos com IgA e impedidos de atravessar a barreira intestinal, mecanismo que ainda não é claro.

Neste trabalho, também foram identificados os nichos intestinais ocupados por esta bactéria determinando a densidade de *Hh* em animais Rag2$^{-/-}$ (imunodeficentes), Ad.col e Nb.col. Os nossos dados após a análise da densidade de *Hh* por qPCR mostraram que a *Hh* está presente em maior densidade no caecum (em geral, 10^4 cópias de 16S de *Hh* por 16S total), de seguida no íleo e cólon (Rag2$^{-/-}$ = ~10^2 cópias de 16S de *Hh*/16S total; B6 Ad.col = ~1 cópia de 16S de *Hh*/16S total; B6 Nb.col = ~10^1-10^2 cópias de 16S de *Hh*/16S total) e em menor número no jejuno (Rag2$^{-/-}$ Ad.col e B6 Nb.col = ~10 cópias de 16S de *Hh*/16S total; B6 Ad.col < 1 cópia de 16S de *Hh*/16S total). Os animais Rag2$^{-/-}$ Ad.col exibiram ainda uma elevada densidade de *Hh* no recto comparativamente aos outros grupos (10^4 cópias de 16S de *Hh*/16S total).

O facto de *Hh* ter sido isolada originalmente a partir do cólon e também do fígado de ratos com hepatite crónica ativa, tumores hepáticos e IBD, motivou a investigação da sua capacidade de atravessar a barreira epitelial intestinal sob as nossas condições experimentais. Dados obtidos anteriormente no nosso grupo sugeriram que *Hh* é capaz de atravessar o epitélio intestinal em ratos B6 Ad.col, indicado pela presença de IgM (primeira Ig a ser produzida por células B maduras) e IgG (produzido mediante hipermutação somática após estimulação) específicos para *Hh* no seu soro. Por outro lado, tínhamos evidências de que a densidade de *Hh* nas fezes em ratos Rag2$^{-/-}$ Ad.col desprovidos de células B e T maduras (mutantes em que a função da enzima que participa na recombinação V(D)J está comprometida, tanto no locus de Ig como no receptor das células T) é maior do que em ratos B6 Ad.col.

Assim, averiguámos se 1) a ausência do sistema imunitário adaptativo e 2) o período de colonização, alteram o tráfico de *Hh* para fora do epitélio intestinal. Para perceber se esta bactéria tem a capacidade de atravessar o epitélio nestas condições experimentais – em animais Rag2$^{-/-}$ Ad.col, B6 Ad.col e B6 Nb.col – a densidade de *Hh* em vários órgãos internos analisada por qPCR. A capacidade de *Hh* atravessar a barreira intestinal permaneceu indeterminada; embora tenha sido verificado um maior número de *Hh* nos MLN de ratos Rag2$^{-/-}$ Ad.col relativamente aos outros grupos, esta bactéria não foi detetada no fígado e baço em nenhum dos grupos analisados. Por outro lado, foram detetadas aproximadamente 10 cópias de 16S de *Hh* por ng de DNA do hospedeiro na GB de ratos B6 Nb.col, mas não em Rag2$^{-/-}$ ou B6 Ad.col. A cultura de *Hh* a partir dos diferentes órgãos internos referidos revelou-se necessária para confirmar ou esclarecer estes resultados.

Finalmente, decidimos comparar o perfil inflamatório destes dois grupos numa situação de disrupção da barreira intestinal. Também investigámos se a colonização com *Hh* promove a progressão da resposta inflamatória no intestino, comparando estes grupos com animais SPF.

Assim, o efeito da colonização com *Hh* numa situação de patologia intestinal foi analisado. Para replicar esta situação foi utilizado um modelo de colite induzida por DSS, avaliando a severidade da inflamação pela perda de peso corporal e pelos níveis de Lcn-2 nas fezes (ELISA) dos animais analisados (n=5 por grupo). Globalmente, uma relativa reprodutibilidade foi verificada entre as duas experiências realizadas independentemente. Como esperado, foi observada uma diminuição gradual do peso a partir do 4º dia do tratamento com DSS em ambas as experiências. No geral, a colonização com *Hh* não afetou o peso dos animais analisados até ao dia 9 (1 dia após ter sido removido DSS).

Na primeira experiência, foi observada uma perda de peso constante até ao 11º dia em todos os grupos; porém, posteriormente, houve uma grande variação entre os ratos B6 Nb.col provocada por 2 animais, que apresentaram uma perda de peso mais drástica. Ainda assim, todos os animais voltaram a ganhar peso sensivelmente a partir dos 12º-13º dias, após o DSS ter sido removido, acabando por recuperar o peso inicial. Na segunda experiência, também foram detectadas algumas diferenças posteriormente ao 10º dia, embora num menor número de dias.

Contudo, os níveis fecais de Lcn-2 não se correlacionaram com o do peso corporal: níveis elevados de Lcn-2 vs recuperação do peso inicial. A regeneração da mucosa intestinal bem como a manutenção da tolerância a *Hh* serão alvo de estudos futuros.

Palavras-chave: *H. hepaticus*; tolerância neonatal; IgA; mono-colonização; tracto GI

ABSTRACT

Helicobacter hepaticus (*Hh*)-newborn colonization in B6 WT mice generates a tolerant response characterized by: undetectable faecal and serum *Hh*-specific IgA, high bacterial loads and maintenance of tolerance until adult life. In this study, monocolonization with this pathobiont revealed that this response is microbiota-independent. Moreover, we demonstrated that the specific Ig produced against *Hh* binds specifically to its surface.

The niches inhabited by this microbe within the mouse GI tract were identified: higher *Hh* loads were found in the caecum followed by colon and ileum and, at lower number, in jejunum. In immunodeficient mice a high *Hh* load was found within the rectum.

Hh ability to traverse the intestinal epithelial barrier remained uncertain as our data was unclear in this respect. Although a higher *Hh* load was estimated within MLN from immunodeficient Ad.col mice, it was not detected within the liver and spleen from any of the groups analysed. Still, we estimated around 10 copies of *Hh* 16S per ng of host DNA only within the GB from B6 Nb.col mice. Culture of *Hh* from the various internal organs is required to confirm these results.

Finally, we investigated the effect of *Hh* colonization in the context of intestinal pathology. DSS-induced colitis was used to model intestinal disease, evaluating the severity of the inflammation. Generally, *Hh* colonization did not affect animal weight; however, the levels of faecal Lcn-2 did not correlate with body weight in both experiments: high Lcn-2 levels vs recovery of the initial weight. Mucosal healing and maintenance of tolerance to *Hh* will be subject for further work.

Keywords: *H. hepaticus*; newborn tolerance; IgA; monocolonization; GI tract

ABBREVIATIONS

Ad.col	Adult-colonized
Ad.mcol	Adult-monocolonized
A647	Alexa 647
AMPs	Anti-microbial Peptides
B6	C57BL/6
bp	Base Pairs
CFU	Colony Forming Units
ELISA	Enzyme-linked Immunosorbent Assay
GB	Gallbladder
Hh	*H. hepaticus*
IBD	Inflammatory Bowel Disease
Ig	Immunoglobulin
ig	intragastric
IgA	Immunoglobulin A
IgA$^-$	IgA-negative
IgA$^+$	IgA-positive
LI	Large Intestine
MLN	Mesenteric Lymph Nodes
Nb.col	Newborn-colonized
Nb.mcol	Newborn-monocolonized
ns	Non-significant
PBS	Phosphate Buffered Saline
PCR	Polymerase Chain Reaction
qPCR	Quantitative Polymerase Chain Reaction
Rag2$^{-/-}$	Recombination Activating Gene 2-deficient
SD	Standard Deviation
SI	Small Intestine
sIgA	Secretory IgA
SPF	Specific-Pathogen-Free; non-colonized with *Hh*
TB	Thyoglicolate Medium
WT	Wild-type

TABLE OF CONTENTS

RESUMO i

ABSTRACT iv

ABBREVIATIONS v

1. INTRODUCTION 1

2. MATERIALS AND METHODS 4

2.1. Mice 4

2.2. GF mice 4

2.3. Colonization and Monocolonization with *Hh* 4

2.3.1. Adult-colonization 4

2.3.2. Newborn-colonization 5

2.4. Monocolonization status confirmation 6

2.4.1. Culture of faecal homogenates in TB Medium 6

2.5. DNA extraction 6

2.5.1. DNA extraction from faecal pellets through a boiling method 6

2.5.2. DNA extraction from samples of intestinal tissue and faeces 7

2.6. *Hh* detection by PCR 9

2.7. Quantification of *Hh* load by qPCR 9

2.8. Detection of Total and *Hh*-specific IgA by ELISA 10

2.8.1. *Hh*-specific IgA detection 10

2.8.2. Total IgA detection 11

2.9. Incubation of faecal extract with cultured *Hh* 11

2.9.1. Faecal extract preparation 11

2.9.2. Incubation 11

2.10. DSS-induced colitis 12

3. RESULTS 13

3.1. Tolerance to *Hh* is microbiota-independent 13

3.2. Validation of Monocolonization and GF status 13
3.3. IgA binds specifically to the surface of *Hh* 14
3.3.1. Incubation of faecal extract with cultured *Hh* 14
3.4. *Hh* distribution throughout the mouse gut 18
3.4.1. *Hh* detection in colonized mice by PCR 18
3.4.2. *Hh* load quantification throughout the mouse GI tract by qPCR 20
3.5. *Hh* ability to traverse the intestinal epithelium 24
3.6. Effect of *Hh* colonization on the progression of intestinal pathology 26
3.6.1. Experimentally-induced colitis in SPF, Ad.col and Nb.col mice 26
4. DISCUSSION 29
5. REFERENCES 36
6. APPENDIX 40
6.1. Original approach of the project 40
6.2. Growth of *Hh* in culture 41
6.3. Faecal extract serial dilution preparation 42
6.4. Primers used in this study 43
6.5. Mice used for *Hh* load analysis by qPCR within the gut and organs 43
6.6. Standards used for qPCR analysis of *Hh* load 44

1. INTRODUCTION

Mammals and other vertebrates are colonized by an abundant and diverse population of commensal bacteria known as the microbiota [8, 16, 22, 42]. The microbiota have coevolved with the host playing key roles on its physiology, namely in tissue development [9, 20] and activation of the immune system.

As the GI tract represents a primary site of exposure to pathogens, the resident microbial community competes with pathogenic organisms restraining their occupation and growth [9, 10, 18]. This mutualistic relationship can be disrupted in individuals with inflammatory bowel disease (IBD) comprising conditions in which chronic inflammation of the GI tract [3, 9] is caused by dysregulated immunity to the microbiota [9, 14], due to changes in the composition of the microbiota [41]. Yet, coevolution of commensals and their hosts contributed to rare inflammatory intestinal immunopathology [4, 12, 13]. Over the last years, an important association between altered microbiota structure and intestinal health in animal models and humans has been stressed and debated.

The intestinal mucosal surface – mucosal firewall – creates a structural and immunological barrier by enhancement of the mucosal barrier function – collective action of mucus, IgA, and AMPs represented in Figure 1 [14]. A reduction in contact between microbes in the lumen and the epithelial cell surface maintains a homeostatic relationship with the microbiota, preventing their entrance into the lamina propria [31, 9, 14]. In the SI, RegIIIγ (antibacterial lectin) plays a key role on this immune mechanism of physical segregation of bacteria from the epithelial surface [31]. Commensals prevent pathogen by induction innate immune responses as well [10, 17]. Various components are involved in maintenance of intestinal homeostasis including the innate immune factors TLRs, the TLR/IL-1R adaptor protein MyD88 and Nod-like receptors (NLRs) [4, 10, 21]. These proteins are responsible for pathogen recognition by the intestinal immune system inducing the production of pathogen-specific IgA, which is T cell-dependent and holds high-affinity [5, 11, 27]. IgA is the major antibody isotype produced at mucosal surfaces and it is essential to mediate intestinal immunity [9, 13, 24] by translocation into the intestinal lumen where it binds and covers the pathogens.

It is still uncertain whether IgA restricts growth of commensals or whether it confines their spread from the intestinal compartment by coating their surface; yet, it is estimated that more than 70% of total immunoglobulin production inside the body consists in secretory IgA [13].

Different niches can be colonized by microbes within a mammalian host such as the skin, intestine, upper and lower respiratory tract, among others. In immunocompetent hosts (i.e., with full immune function) internal organs are usually retained sterile, unlike other niches as the colon or skin that are colonized by endogenous microbiota [15]. Upon colonization immediately after birth, the intestinal mucosa and the gut-associated lymphoid tissues such as Peyer's patches, isolated lymphoid follicles (ILFs) and mesenteric lymph nodes (MLN), engage in a maturation process [14, 42].

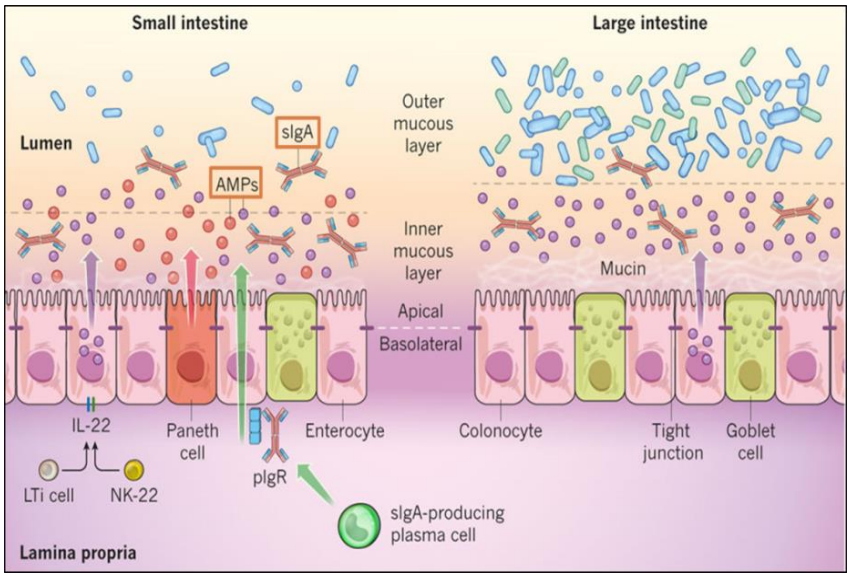

Figure 1. Intestinal epithelial barrier function. Specialized cells at the base of the SI sense the microbiota inducing the production AMPs. High concentration of AMPs and commensal-specific sIgA impair bacterial colonization or penetration. In the LI, the microbiota induce the production of mucins, main components of the inner mucus layer Adapted from Maynard *et al.* (2012).

As a model of a host-microbe interaction, different studies involving colonization of mice with *Helicobacter hepaticus* (*Hh*) were developed by our group (unpublished data). *Hh* is a spiral form and bipolar, single, sheathed flagella, microaerophilic bacterium included in Gram-negative bacteria. *Hh* was first isolated from the liver, caecal and colonic mucosa of infected inbred strains of A/JCr mice in the 90s [7], associated to chronic active hepatitis, IBD and liver tumours [1, 6, 7]. There is evidence of *Hh* prevalence both in the wild and in laboratory mouse colonies [32, 34, 39, 44]. Unlike hepatitis-prone A/JCr, C57BL/6 mice are rapidly colonized and show resistance to *Hh*-associated disease [44]. There is natural transmission from mother to newborns, and between adults allied to the innate behaviour of coprophagia – effective colonization between co-housed mice [40, 44]. This microbe establishes a long-term colonization in WT mice without causing intestinal disease [32, 36], although it can cause chronic colitis in immunocompromised mice, particularly in immunoregulatory cytokine interleukin-10 (IL-10)-deficient mice [32, 35-37].

In previous work developed in our group, *Hh*-newborn colonization in B6 WT mice promoted generation of a tolerant response characterized by: undetectable faecal and serum *Hh*-specific IgA, high bacterial loads and maintenance of tolerance until adult life (unpublished data).

Given this evidence, our aim was to explore whether besides *Hh*, other bacteria of the intestinal microbiota share this tolerogenic potencial induced upon newborn-colonization or whether it is the result of a selected mouse-*Hh* mutualistic relationship. Due to various difficulties explained in the Appendix section (6.1.) our aims were re-evaluated. Instead, we decided to explore further the ecological context from the microbe, *Hh*, perspective. Notably, in this project we dissected the relevance of certain features from the surrounding (intestinal) microenvironment.

One of the features evaluated was the physiology of the immune response towards *Hh*, proving that the Ig produced specifically against *Hh* binds directly to its surface.

Later, we explored the influence of a complex microbiota in this response to *Hh*, revealing that the tolerant response to *Hh* induced when animals are colonized as newborns is a phenomenon independent of the remaining intestinal bacteria that reside in the mouse GI tract.

As *Hh* colonizes the mucosa of colon and caecum, the spatial topography of this compartment – which areas of the mouse GI tract are colonized by *Hh* and where it colonizes in higher burden – were analysed in different types of hosts (immunodeficient, colonized at adult age, colonized within the neonatal stage of life). In addition, we assessed whether *Hh* colonizes other organs of the host or if it remains confined within the different intestinal surroundings.

Lastly, we evaluated the effect of *Hh* colonization in the context of intestinal pathology, in which there is the mucosal firewall is damaged.

2. MATERIALS AND METHODS

2.1. Mice

SPF (free of certain pathogens) B6 WT and Rag2$^{-/-}$ (lacking mature B and T lymphocytes) mice were bred and maintained at the Instituto Gulbenkian de Ciência SPF Animal house (Rodents) facility and were manipulated in accordance with the Instituto Gulbenkian de Ciência ethical committee. Animals were age- and sex-matched in all the experiments; SPF B6 and Rag2$^{-/-}$ mice were transferred into a specific experimental room where *Hh* colonization was performed routinely and colonized animals were maintained.

2.2. GF mice

GF B6 mice were bred and maintained at Instituto Gulbenkian de Ciência GF Animal house (Rodents) facility and were manipulated in accordance with the Instituto Gulbenkian de Ciência ethical committee. These were regularly tested for sterility by culture of faecal homogenates in TB medium (REF 211260, Lot 3113449, BD BBL^{TM} Fluid). All experiments using GF animals were conducted inside a laminar flow ISOcage Biosafety Station (IBS) (Tecniplast; GF Facility, Instituto Gulbenkian de Ciência) in order to maintain sterility. ISOcages enable total isolation using a HEPA filter and a seal safe system. ISOcages were exclusively opened and closed inside the IBS cabinet. After the ISOcage was closed, it was returned to an appropriate air flow system rack. Upon experimental procedures, fresh Virkon S disinfectant was prepared and all surfaces and materials were vigorously sprayed and disinfected for two minutes before introduction into the IBS. A Virkon chamber connected to the IBS allows decontamination of the outer side of the ISOcages holding the GF mice. Every time the handler left the IBS to place another ISOcage inside the Virkon chamber, the extra pair of gloves was sprayed with Virkon S again, followed by two minutes of disinfection prior to animal manipulation.

2.3. Colonization and Monocolonization with *Hh*

2.3.1. Adult-colonization

8 weeks old B6 WT mice (either conventionally reared in SPF or GF conditions; Figure 1, 1 and 3) were submitted to ig colonization with 100 µl of faecal bacteria suspension prepared from faeces from a *Hh*-positive B6 colonized/monocolonized with cultured *Hh* (protocol in Appendix section, 6.2.). Faecal pellets were collected and homogenized in sterile PBS (500 µl PBS/pellet) using a syringe plunger. The faecal homogenate was filtered with a 100 µM Falcon cell strainer (BD Biosciences) to remove larger particles and transferred into a clean 2 ml tube using a sterile disposable Pasteur pipette.

Animals were inoculated with 100 µl of the filtered homogenate using a sterile syringe coupled with a silicone tip needle (sterile-single use animal feeding needle, size: 20Gx1.5'', Cadence Science). Ad.mcol (Ad.mcol) animals were kept under sterile conditions throughout the experiment.

2.3.2. Newborn-colonization

9 weeks old B6 WT mice (either conventionally reared in SPF or GF conditions; Figure 2, scheme 2 and 4) were born from colonized/monocolonized mothers. Nb.mcol animals were kept in sterile conditions throughout the experiment. Because *Hh* is naturally transmitted from mother to neonates, we were able to produce *Hh*-positive litters colonized after birth. Colonization was confirmed by PCR of DNA purified from faecal samples (boiling method) from colonized animals using *Hh* 16S rRNA specific-primers (Appendix, 6.2.).

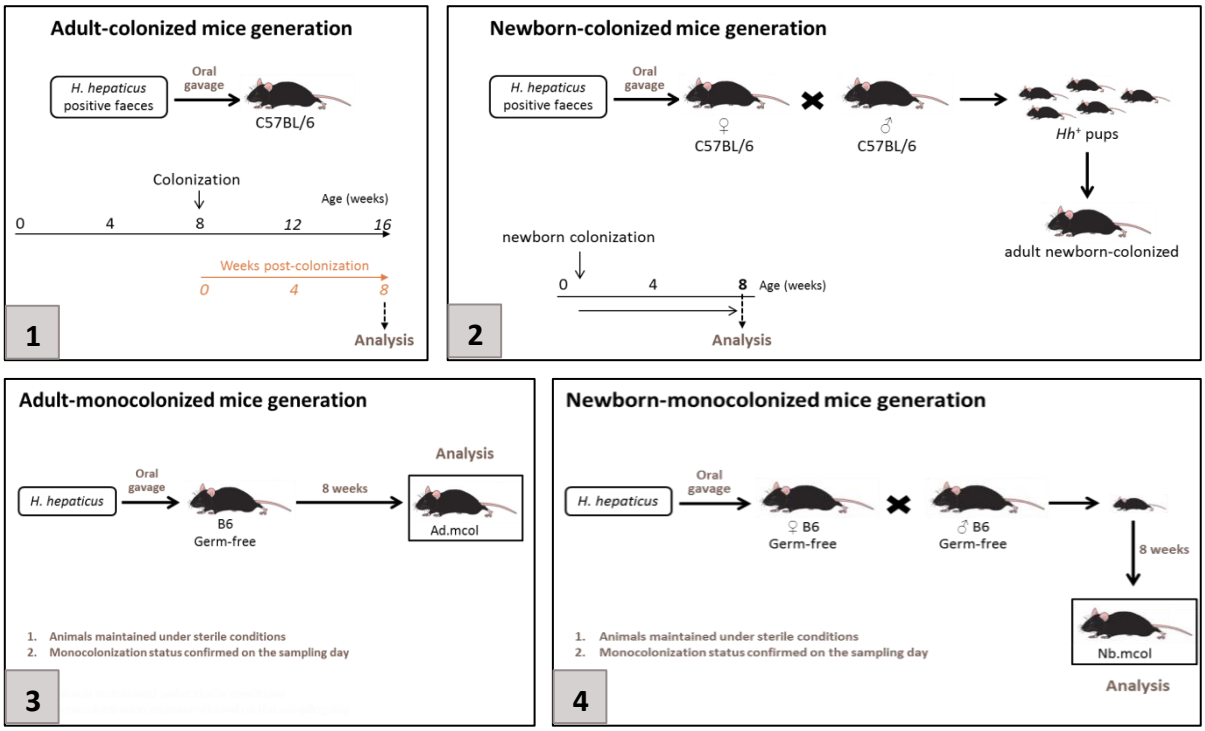

Figure 2. Experimental setting of Colonization and Monocolonization with *Hh*. (1) Experimental approach used for generation Ad.col mice (analysed 8 weeks post-colonization – 16 weeks old mice). (2) Generation of Nb.col mice (born from previously *Hh*-**colonized mothers** – analysed at 8 weeks of age). (3) Generation of Ad.mcol mice (analysed 8 weeks post-colonization – 16 weeks old mice). (4) Generation of Nb.mcol mice (born from previously *Hh*-**monocolonized mothers** – analysed at 8 weeks of age). Animals were analysed as adults independently of the colonization context.

2.4. Monocolonization status confirmation

2.4.1. Culture of faecal homogenates in TB Medium

In addition to the sterility tests performed upon the transfer of GF mice to the experimental room, we performed an additional test.

To confirm monocolonization and GF status of manipulated mice, we cultured faecal homogenates from each manipulated mouse followed by incubation for 7 days. Bacterial growth was assessed by turbidity of the medium after incubation. As a positive control, we cultured a faecal sample from a B6 SPF mouse; as a negative control of bacterial growth, we incubated only TB medium, manipulated with a sterile Pasteur pipette. We prepared fresh TB medium (BD BBL^{TM} Fluid, REF 211260, Lot 3113449) adding MiliQ water to the powder in a shot flask. Then we stirred the flask until the powder was dissolved, and autoclaved for 1h. After autoclaving, the flask was stirred and left at RT overnight. The next day, a purple phase was seen on the top and a yellow/orange at the bottom of the flask (aerobic and anaerobic phases, respectively). Before usage, we mixed the medium to homogenize both growth phases. All procedures described below were executed inside a vertical flow hood in order to avoid environmental contamination of our samples. We added 4 ml of TB medium into 15 ml Falcon tubes. Each faecal pellet, collected into 1.5 ml tubes, was homogenized in 1 ml of TB medium using a disposable Pasteur pipette. The faecal homogenate was centrifuged at 16000xg for 5 minutes, and the supernatant was removed and homogenized in the Falcon tube containing the fresh TB medium. All samples were incubated at 37°C, for 7 days.

2.5. DNA extraction

2.5.1. DNA extraction from faecal pellets through a boiling method

Two solutions were prepared preceding the extraction process (protocol adapted from [45]). An alkaline lysis reagent was prepared by dissolving NaOH and disodium EDTA in distilled water, making a 25 mM NaOH/0.2 mM EDTA solution with an unadjusted pH of 12. An acidic Tris HCl buffer was prepared by dissolving Tris HCl in distilled water, making a 40 mM Tris HCl solution with an unadjusted pH of 5.

Faecal pellets were collected into 2 ml tubes (two small faecal pellets or just one big size pellet). After feces collection, 700 µl of the first described solution (NaOH/EDTA) were added to the tubes. The tubes were heated at 95°C for 3 minutes on a Thermomixer (Thermomixer comfort, Eppendorf) and then homogenized on a vortex mixer for 30 seconds. The heating step was repeated once more (95°C), for 5 minutes, followed by homogenization on a vortex mixer

for 30 seconds (the faecal pellets must be dissolved). Next, the tubes were centrifuged at 14000 rpm, for 2 minutes. After centrifugation, 50 µl of the supernatant (avoiding solid contaminants) were placed in a new Eppendorf tube containing 50 µl of the second solution described (Tris HCl), and mixed gently. All DNA samples were stored at -20°C or used immediately for PCR using 2 µl of each sample.

2.5.2. DNA extraction from samples of intestinal tissue and faeces

Conventionally reared SPF B6 WT mice were submitted to either adult- (n=13) or neonatal-colonization (n=12) with *Hh.* SPF B6 Rag2$^{-/-}$ mice were colonized with *Hh* as adults (n=4) and controls were maintained in SPF conditions (n=2) (Appendix, 6.5.). Genomic DNA was purified from 1 faecal pellet, different compartments of the GI tract and a number of organs using a commercial kit (NZY Tissue gDNA Isolation kit, nzytech genes & enzymes MB13502, modified for DNA extraction from faeces, including an initial step of 95°C incubation).

Faecal pellets were collected into 1.5 ml tubes adding 180 µl of NT1 buffer and left soaking for about 30 minutes.

In the meantime, liver and spleen (Figure 3, B) specimens were isolated using forceps and placed into a cell culture dish 60 x 15 mm (standard growth surface for adherent cells, red, SUREGrip Design, sterile, pyrogen-free, non-cytotoxic, REF 83.3901.500; Sarstedt). We added 2 ml of sterile PBS into the dish containing the liver and 1 ml to dish containing the spleen and shattered the organs using a nylon mesh and the back side of a sterile 5 ml syringe plunger (5cc Luer Slip Tip Syringe without Needle, catalogue number SS-05S; Terumo). Organ homogenates were transferred into a 15 ml Falcon tube using a disposable plastic Pasteur pipette. We washed the dish and the nylon mesh with an additional 1 ml PBS in order to transfer all the shattered tissue. The Falcon tubes were centrifuged at 450G for 5 minutes and 2 ml of supernatant were removed into a clean 2 ml tube. The 2 ml tubes were centrifuged at 3000G for 15 minutes (RT) and the supernatant was discarded, and the pellet re-suspendend in 180 µl of NT1 buffer.

MLN and GB were collected with forceps and placed directly in 180 µl NT1 buffer.

Intestinal tissue samples – duodenum, jejunum, ileum, caecum, colon and rectum – depicted in (Figure 3, A) were collected by cutting ~1 cm of tissue with surgical scissors, opened longitudinally and washed in PBS in individual cell culture dishes; then cut into smaller size pieces with a surgical scissors and placed in 180 µl of NT1 .

After this, the samples were heated for 3 minutes at 95°C on a Thermomixer (Thermomixer comfort, Eppendorf) and mixed vigorously by vortex to homogenize well. Then the samples were heated again for 5 minutes at 95°C. After this initial step of incubation, the samples doing a slight spin at 0.1G for 30 seconds and left on the bench for 5 to 10 minutes to cool. Then we added 25 µl Proteinase K solution and mixed by vortex at mid rotation (1800 rpm). The samples were incubated at 56°C overnight (~14h) with shaking (750 rpm).

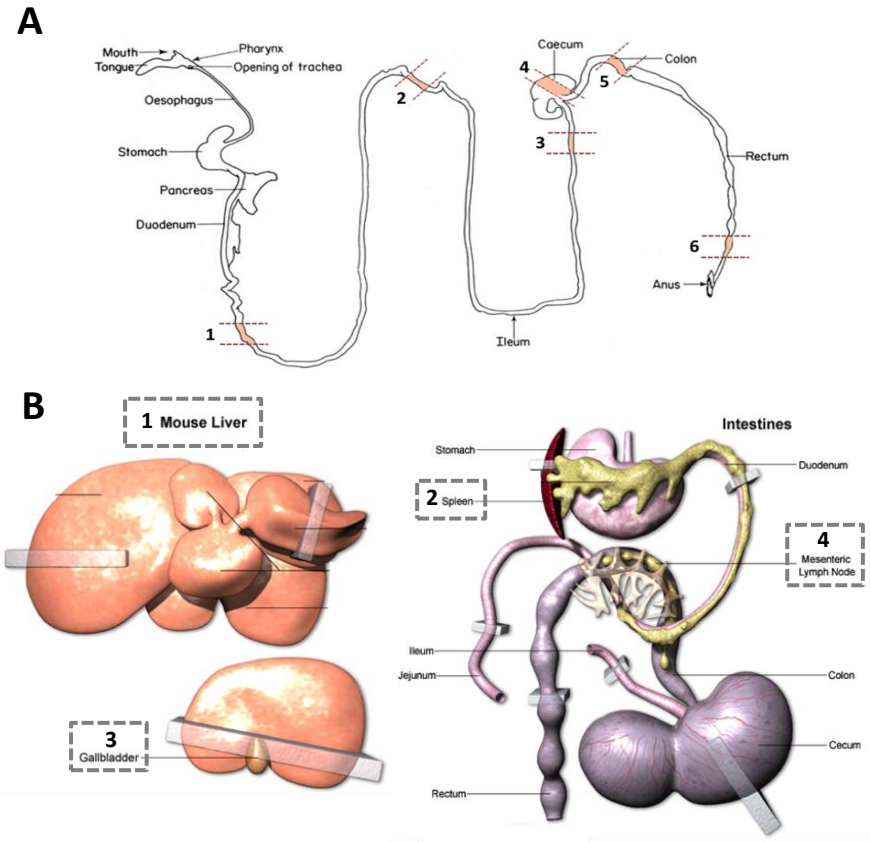

Figure 3. Mouse GI tract and visceral anatomy. (A) For *Hh* load determination throughout the mouse GI tract we isolated different areas (defined by 2 dashed orange lines): duodenum (1), jejunum (2), ileum (3), caecum (4), colon (5) and rectum (6). (B) For determination of *Hh* traversing towards other organs we have isolated the liver (1), spleen (2), GB (3) and MLN (4). A[46], B[47].

For intestinal tissue/organ samples, some of the steps from the manufacturer instructions were changed namely, in the buffer NL step we added 300 µl, transferring 200 µl of supernatant into 200 µl of 100% ethanol. In the step of pre-heated NE buffer addition, for tissue/organ samples we added 25 µl of sterile distilled H_2O following the instructions of the protocol.

Following the DNA extraction protocol, we measured the DNA concentration of all samples using NanoDrop 2000 UV-Vis Spectrophotometer (Thermo Scientific). Each sample was measured twice.

2.6. *Hh* detection by PCR

To confirm *Hh*$^+$ colonization, we extracted DNA from 1 faecal pellet from each animal using the boiling method described above, and assessed *Hh* incidence by PCR using *Hh*-specific 16S rRNA primers (417 bp product; Appendix, 6.4.).

For the PCR mix preparation we used 1.25 mM $MgCl_2$, 200 µM dNTP, 5x green GoTaq buffer, 0.4 µM forward and 0.4 µM reverse primer, 5U/µl GoTaq (GoTaq® G2 Flexi DNA Polymerase, Promega), 2 µl of DNA template from each sample and added distilled sterile water (Gibco™ by life technologies, catalogue number 15230-001) up to a total volume of 25 µl. The cycling conditions used for *Hh*-specific 16S detection were an initial denaturation of 94°C for 5 minutes, 36 cycles of 94°C for 30 seconds, 60°C for 45 seconds and 72°C for 1 minute, final extension of 72°C for 10 minutes and a hold at 4°C for 30 minutes.

All PCR reactions were executed in a thermal cycler (Bio-Rad MyCycler™ Personal Thermal Cycler) using a 25 µl algorithm measurement. PCR products were ran in 2% agarose (SeaKem® LE Agarose 500 g; catalog number 50004, Lonza) gels 0.5% Red Safe [Nucleic Acid Staining Solution, 1ml (20 000:1), catalogue number 21141; SBS Genetech] and visualized in Gel Doc™ XR (Molecular Imager Gel Doc™ XR Imaging System; BIORAD). Correct product size was assessed using a DNA ladder (50-1500 bp, DNA Ladder VI; NZYTech). As a positive control, we used DNA (50 ng/µl) purified from *H. hepaticus* grown in culture; as an internal amplification control, we used 18S rRNA (Appendix, 6.4.) primers; since all samples were retrieved from mice, we sought to use host DNA as an internal amplification control from that point on.

2.7. Quantification of *Hh* load by qPCR

Relative quantification of *Hh* 16S DNA was determined by qPCR analysis, using *Hh*-specific 16S rRNA primers (Appendix, 6.4.). The number of *Hh*-specific 16S rRNA copies was normalized to the number of total 16S copies present within each sample. The relative abundance of this bacterium was determined using standard curves constructed with reference to cloned bacterial DNA corresponding to the segment (417 bp; pGEM-T Easy vector (Promega) + 417, 1:1000, 2.69E+08 copies/ng) of the 16S rRNA gene amplified using *Hh*-specific 16S rRNA primers and to the segment of the 16S rRNA gene amplified using

Eubacteria – Universal – primers in *E. coli* DNA (1.40E+06 copies/ng) (Appendix, 6.4., 6.6.).

To determine *Hh* load throughout the mouse GI tract, liver, spleen, GB and MLN, the number of *Hh*-specific 16S rRNA copies was normalized to ng of mouse (host) DNA – 18S rRNA gene – (Appendix, 6.4., 6.6.). Because we did not know how many copies of 18S rRNA gene are present in host cells we used 10 fold dilutions of the described DNA sample (Appendix, 6.6.). The qPCR conditions used were 5 units/µl of SYBR Green 2x (iTaq™ Universal SYBR® Green Supermix, BIORAD), 0.5 units/µl of forward primer 10 µM, 0.5 units/ µl of reverse primer 10 µM, 2 units/µl of distilled sterile water (Gibco™ by life technologies, catalogue number 15230-001) and 2 µl of DNA template. All primer sets were diluted on the day of the qPCR plate preparation.

For accurate determination of the DNA concentration of our samples, we used Qubit Fluorometric DNA Quantitation kit (Qubit® 2.0 fluorometer, catalogue number Q32866; Invitrogen by life technologies), selecting the dsDNA "Broad range" option. For each sample measurement we used 1 µl DNA, using a previous 1:200 dilution (199 µl buffer to 1 µl dye). qPCR was performed in 384-well plates using a CFX384 thermal cycler (CFX384 Touch™ Real-Time PCR Detection System; BIORAD). Each sample was replicated 3 times. For every qPCR mix, we used non-template controls (NTC), in which no DNA was added (just the qPCR mix). The qPCR for *Hh* load quantification in intestinal tissue and the one for organ tissue samples were performed independently.

2.8. Detection of Total and *Hh*-specific IgA by ELISA

2.8.1. *Hh*-specific IgA detection

Faecal extracts from mice were prepared by homogenization of faecal pellets in PBS containing a protease inhibitor cocktail (PIC; catalogue number P8340; Sigma-Aldrich) at approximately 100 µl/10 mg. For this, we added 500 µl of PBS+PIC to each sample. After soaking for 1h, the tubes were centrifuged at full speed (16000G) for 10 minutes in order to clear the supernatant. Bacterial antigens were prepared by cultured bacteria re-suspension in PBS, lysing in french press, centrifuging to remove insoluble particles, and quantifying protein content by Bradford Protein Assay. ELISA plates were coated overnight with bacterial antigens, washed 3 times in PBS0.05%Tween20, and blocked with PBS2%BSA for 2h before addition of mice faecal extracts. After faecal extract incubation overnight, plates were washed 3 times in PBS0.05%Tween20, incubated for 1.5h with the Goat Anti-Mouse IgA-UNLB (unlabelled) capture antibody (stock at 1 mg/mL, catalogue number 1040-01, Southern Biotech) and washed 3 times in PBS. TMB was added to plates and the reaction was stopped after approximately 2 minutes (until standard fourth

dilution turned blue) with 0.1M H_2SO_4. Finally, absorbance at 450 nm was read using Victor 3 Plate Reader (PerkinElmer).

2.8.2. Total IgA detection

ELISA plates were coated overnight with Goat Anti-Mouse IgA-UNLB, washed 3 times in PBS0.05%Tween20, blocked with PBS2%BSA for 2h before addition of mice faecal extracts. After faecal extract incubation overnight, plates were washed 3 times in PBS 0.05% Tween20, incubated for 1.5h with the Goat Anti-Mouse IgA-HRP (Horse-radish protein) detection or secondary antibody (1:4000 dilution, catalogue number 1040-05, Southern Biotech)and washed 3 times in PBS. TMB was added to plates and the reaction was stopped after approximately 2min with 0.1M H_2SO_4. Absorbance at 450 nm was read.

2.9. Incubation of faecal extract with cultured *Hh*

2.9.1. Faecal extract preparation

We collected 1 faecal pellet from 2 different animals within each group into a 1.5 ml tube. We collected faecal pellets from SPF (n=3), 2 Ad.col (n=5) and 2 Nb.col (n=5) mice in order to evaluate the IgA^+ bacteria profile upon the distinct time of colonization with *Hh*. To prepare the faecal extracts, we homogenized each faecal pellet in 500 µl of cold filtered (0.2 µm) PBS by vortex. Faecal homogenates were centrifuged at 16000G for 5 minutes and 320 µl of supernatant were removed into a clean 1.5 ml tube and centrifuged once more at 16000G for 5 minutes. Finally, 300 µl of supernatant were removed into a clean 1.5 ml tube. For every sample, faecal extract serial dilutions were prepared on a plate (Appendix, 6.3.). Here, we used 10 µl of undiluted faecal extracts from SPF, Ad.col and Nb.col animals and prepared 3 serial dilutions (1:3, 1:9 and 1:27).

2.9.2. Incubation

We used *Hh* grown in culture bacterial suspension with 2.70E+10 CFU/ml (provided by Margarida Parente, Molecular Genetics of Microbial Resistance, ITQB, Oeiras) as described in Appendix (6.2.). We slightly homogenized and washed the initial *Hh* bacterial suspension. For incubation with faecal extracts, we added 20 µl of *Hh* bacterial suspension ($1x10^6$ CFU) into each well of the dilution plate. Then, we sealed the plate and incubated at 4°C for 30 minutes. The volume of each well was then transferred into clean 1.5 ml tubes. Then we

added 500 µl PBS and centrifuged at 12000G for 5 minutes. The resulting pellet was re-suspended in 20 µl of anti-IgA-A647 (Goat Anti-Mouse IgA, catalogue number 1040-01, Southern Biotech; labelled with Alexa 647 at Instituto Gulbenkian de Ciência by the Antibody service) at 1:200 in PBS, and incubated 15 minutes on ice. We washed the staining by adding 500 µl PBS and centrifuged at 12000G for 5 minutes. Finally, we re-suspended the pellet in 300 µl of PBS + Syto 9 1:600 (Syto 9 green fluorescent nucleic acid stain, 3.34 mM solution in DMSO, Live/Dead Bac Light™ Bacterial Viability and counting kit, L34856 Lot 1099894, Molecular Probes, Invitrogen). In parallel, we also prepared negative controls, in which we added only Syto 9 to 20 µl of bacterial suspension, and anti-IgA-A647 + Syto 9 to 20 µl of bacterial suspension following the same incubation and washing protocol.

2.10. DSS-induced colitis

Animals were sex- and age-matched both in the first and second DSS experiments.

To model intestinal disease in our animals, we induced colitis in B6 SPF, adult-colonized and newborn-colonized mice (n=5 per group) by adding a 3% (w/v) solution of dextran sodium sulfate (DSS; molecular weight: 36000–50000 Da; MP Biomedicals) to the drinking water of the animals. In order to induce acute colitis we changed DSS every other day. At day 8, DSS was removed and animals were given regular water to recover from inflammation; protocol adapted from [25]. Faecal pellets were collected at days 1, 5, 11 and 18. Animal weight development was recorded at day 0 (before adding DSS), day 3, 5, and from this point on, every day until animals recovered the initial weight. Animals were weighed on a precision scale inside a big size plastic beaker that was disinfected with Virkon S and ethanol; SPF mice were always weighed first. Immediately after placing the animals inside the plastic beaker, these responded by freezing and their weight was recorded.

The severity of the Intestinal inflammation was assessed as following: body weight loss until DSS removal and recovery of the initial weight; measurement of lipocalin (Lcn-2) levels in faeces by ELISA [3] at the onset of the DSS treatment and until the end of the experiment (d0, d5, d11, d18).

3. RESULTS

3.1. Tolerance to *Hh* is microbiota-independent

Given the tolerogenic potential of *Hh* upon newborn-colonization, we investigated the impact of the gut microbiota on this response. To determine whether *Hh*-induced tolerance is dependent on the presence of a normal and complex microbiota, we performed monocolonization (exclusively with *Hh*) experiments in GF mice. Ad.mcol (Figure 1; 3, Ad.mcol) animals were generated by oral gavage of 8 weeks old B6 GF mice with *Hh*-positive feces from B6 mice previously monolonized with cultured *Hh*. These were analysed 9 weeks post-colonization. Nb.mcol (Figure 1; 4, Nb.mcol) were born from B6 monocolonized mothers, and analysed at 9 weeks old. Both animal groups were kept in sterile conditions throughout the experiment to avoid contamination with other bacteria. After confirmation of *Hh* colonization – detection of *Hh* 16S in faeces by PCR –concentration of faecal IgA was assessed by ELISA of faecal extract from each animal.

3.2. Validation of Monocolonization and GF status

To confirm monocolonization and GF status of our animals, we cultured faecal homogenates from each mouse in TB medium. When mice were manipulated for faecal sample collection, we collected an additional pellet from each animal. The additional faecal pellet was homogenized and cultured in TB medium later (data not shown; protocol described in Materials and Methods, 2.5.). Upon generation of *Hh*-monocolonized mice, we maintained B6 GF animals (n=3) in parallel until the end of the experiment. Because monocolonization and maintenance of GF animals is a very challenging experimental setting prone to contamination, single colonization and sterility confirmation, respectively, was required. As *Hh* is a microarephilic bacterium that requires very specific growth conditions not reproduced in these TB cultures, any sign of turbidity detected in our samples would undoubtedly correspond to contamination. Indeed, after incubation for 7 days (37°C) no bacterial growth was detected in our samples, i.e., the TB medium was clear as the negative control (TB medium only; data not shown). Conversely, in the positive control (faecal homogenate from a SPF animal) the turbidity of the medium was evidently visible (data not shown). This sterility test allowed the validation of single colonization with *Hh* and GF status, thus, making sure that the specific-antibody titres measured on either Ad.mcol or Nb.mcol mice were a consequence of the colonization with this bug.

Similarly to what was seen by our group for B6 SPF Ad.col mice (unpublished data), in Ad.mcol mice we detected a strong anti-*Hh* IgA response (Figure 4, A and B; Ad.mcol). In contrast, in faecal extracts from Nb.mcol animals, anti-*Hh* IgA was not detected (Figure 4, A and B; Nb.mcol). This *Hh*-specific IgA profile

similar to SPF animals suggests that the tolerant response elicited by this bacterium is microbiota-independent, i.e., the tolerogenic potential of *Hh* induced when animals are colonized as newborn does not require the presence of other intestinal commensal bacteria. Anyhow, the total faecal IgA titre from Ad.mcol mice was considerably lower, compared to SPF Ad.mcol mice (Figure 4, C; Ad.mcol; median).

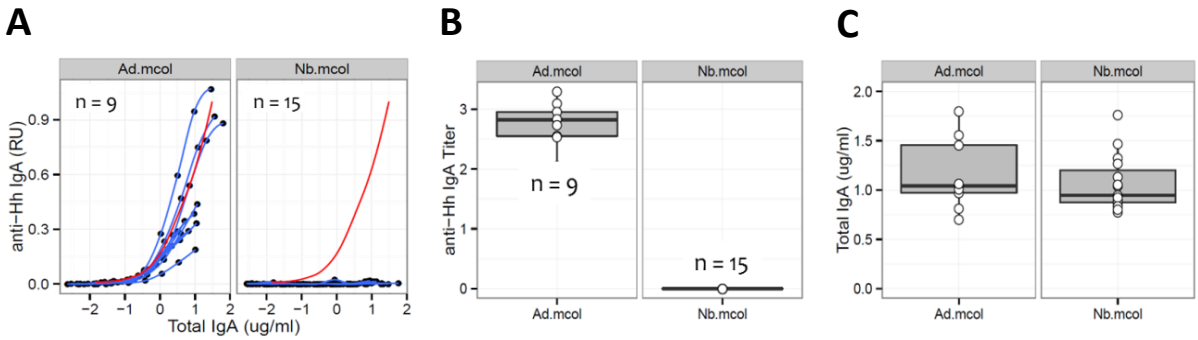

Figure 4. Tolerance to *Hh* is microbiota-independent. (A) Faecal anti-*Hh* IgA (RU – relative units) vs Total IgA (µg/ml of faeces). A pool of faecal extracts from SPF Ad.col mice was used as a reference for *Hh*- specific IgA (red curve). Animals were kept under sterile conditions throughout the experiment. *Hh*-specific IgA (B) and Total IgA (C) titres in faeces (ELISA). Ad.mcol: 8 weeks old B6 GF mice were colonized with *Hh*-positive faeces from B6 mice monolonized with cultured *Hh*, and analysed 9 weeks post-colonization. Nb.mcol: 9 weeks old B6 mice born from monocolonized mothers. N indicated on the graphs. The graphs shown were executed on R software.

3.3. IgA binds specifically to the surface of *Hh*

3.3.1. Incubation of faecal extract with cultured *Hh*

As it was presented above, we often used ELISA assays to evaluate whether *Hh*-specific IgA is present in faecal samples from mice submitted to different colonization conditions. This technique allowed us to detect a robust Ig response directed to *Hh* (high titre of anti-*Hh* IgA) in Ad.mcol mice in contrast to the other experimental groups. To understand how IgA interacts with *Hh* bacterial cells *in vivo*, we incubated faecal extracts from the different experimental groups with *Hh* bacteria grown in culture.

We incubated serially diluted faecal extracts from B6 SPF, Ad.col and Nb.col mice with a cultured *Hh* bacterial suspension; $1x10^6$ CFU (provided by Margarida Parente, Molecular Genetics of Microbial Resistance, ITQB, Oeiras). SPF mice were used as negative controls, for which the IgA-positive bacterial population was expected to be absent *a priori*. A 30 minutes incubation ensured binding of faecal IgA antibodies present in each sample to the bacterial

antigens, followed by staining with an anti-IgA-A647 and Syto 9 in order to detect the proportion of IgA-coated bacteria.

In addition, 2 stain controls were used to ensure the detection of anti-IgA-A647 specific binding to IgA-coated *Hh* after incubation: simply cultured *Hh* bacteria stained with anti-IgA-A647 + Syto 9, and with Syto 9 only (Figure 5, D and E respectively). These stain controls were used to demonstrate that the IgA-positive population in our samples is, in fact, the result of anti-IgA labelled antibody specific binding to the IgA-coated *Hh*. The gating strategy used to detect the IgA-coated *Hh* included the following steps: first, we excluded doublet bacterial cells using the Pulse width parameter, which determines the particle diameter when cells are passing through the laser beam. Thus, we gated the population with low Pulse width and high Syto 9 fluorescence (Figure 5, A); then, we exluded dead bacterial cells by gating the previously selected population in Side Scatter vs Syto 9 (Figure 5, B) – gating the Syto 9^{high} population limited our analysis for only live bacteria (the fluorescence for this nucleic acid stain is proportional to the amount of DNA inside the cell, which is higher in live bacteria); finally, after selecting the live bacteria, the IgA-coated population was defined within Syto 9 vs IgA (Figure 5, C).

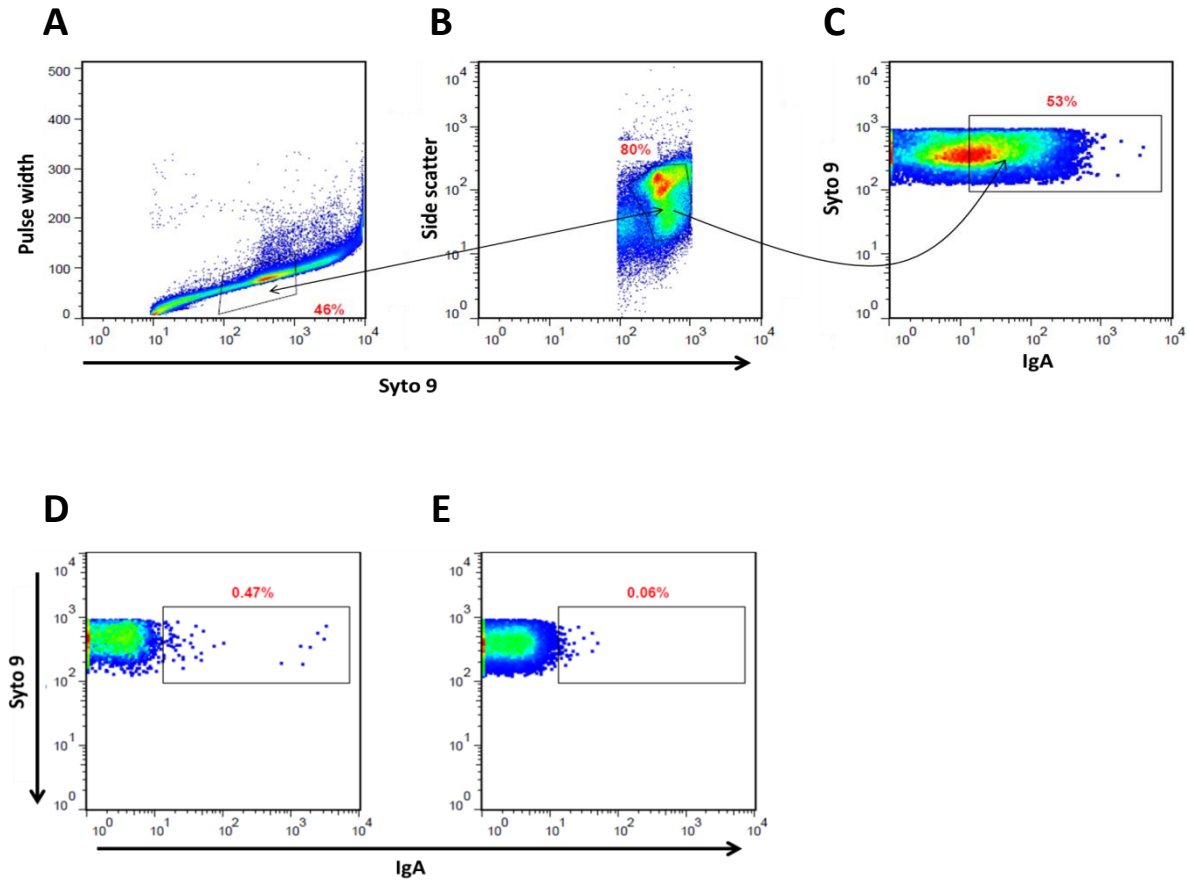

F

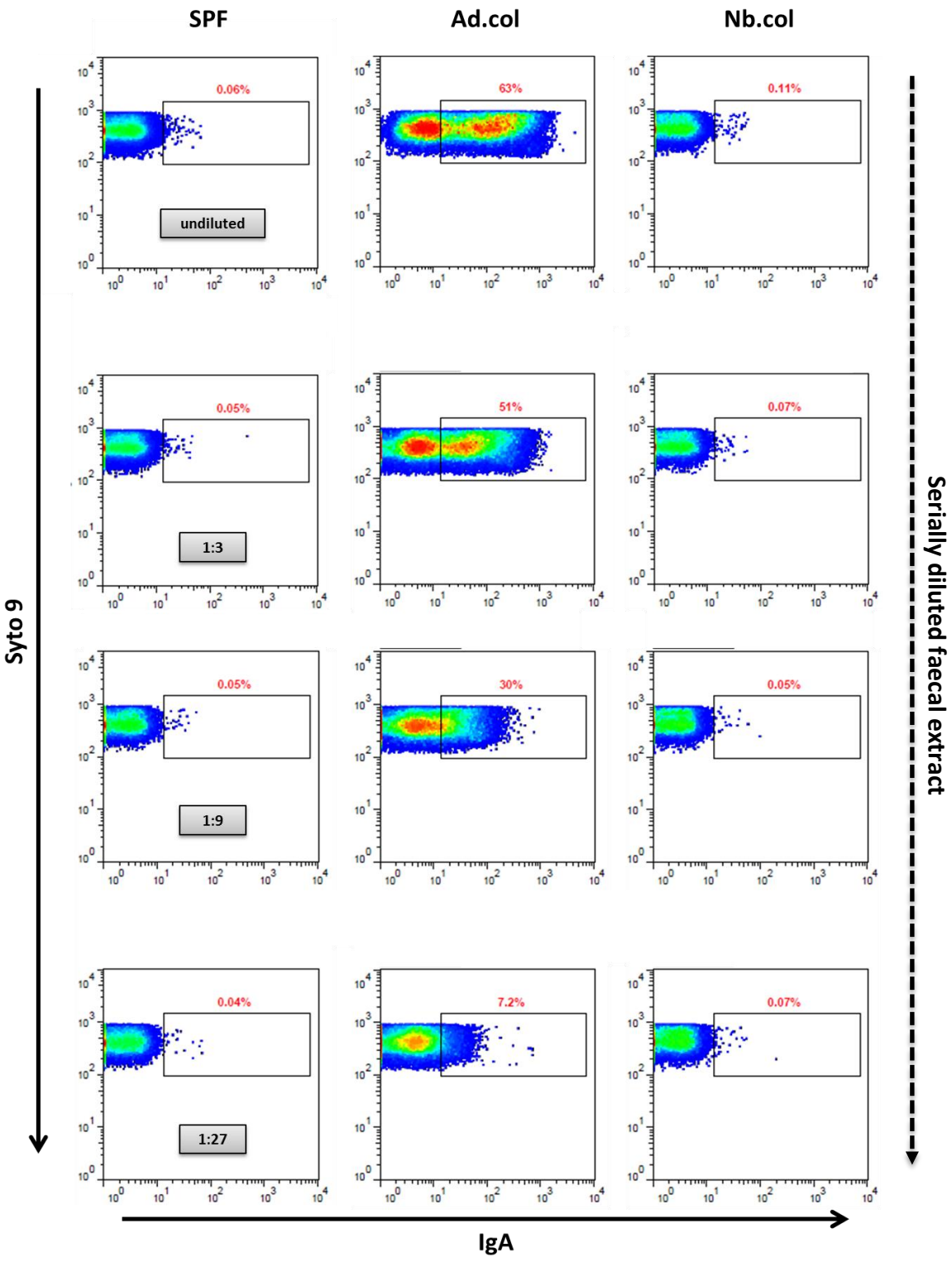
SPF
Ad.col
Nb.col
0.06%
63%
0.11%
undiluted
0.05%
51%
0.07%
1:3
0.05%
30%
0.05%
1:9
0.04%
7.2%
0.07%
1:27
Syto 9
IgA
Serially diluted faecal extract

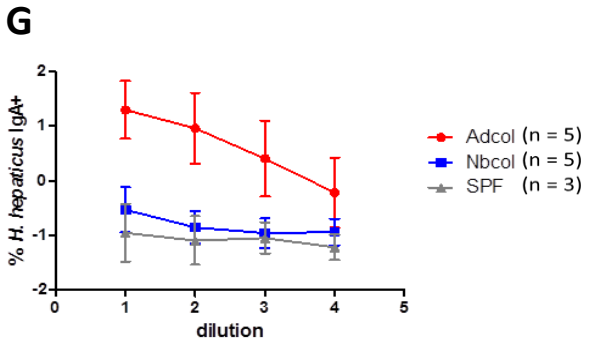

Figure 5. IgA binds specifically to the surface of *Hh*. Faecal extracts from SPF B6, Ad.col and Nb.col mice were incubated with cultured *Hh* ($1x10^6$ CFU). Gating strategy used (represented by undiluted faecal extract from an Ad.col mouse): 1) doublet exclusion (A); 2) exclusion of dead bacterial cells (B); 3) restriction to the IgA^+ population (C). Quality stain controls: cultured *Hh* stained with anti-IgA-A647 + Syto 9 (D) and with Syto 9 only (E). (F) Faecal IgA^+ population profile representing each experimental group decreases according to the dilution factor (undiluted; 1:3; 1:9; 1:27). (G) Proportion of *Hh* IgA^+- population within each group across serial dilutions. The results shown are representative of 2 independent experiments (analysed on FACS Calibur and CyAN^{TM} ADP flow cytometers; Flow Cytometry Unit, Instituto Gulbenkian de Ciência). Flow cytometric analysis was done in FlowJo software.

Flow cytometric analysis revealed that the proportion of IgA-positive bacteria in undiluted faecal extracts exhibited Ad.col mice with *Hh*, compared to either SPF or Nb.col mice (Figure 5, F; SPF = 0.06%; Ad.col = 63%; Nb.col = 0.11%; representative from each experimental group) as it had been observed previously in our lab (unpublished data). We were able to detect the IgA-positive population under serial dilutions of faecal extract from Ad.col animals, which decreases consistently according to the dilution factor (Figure 5, F; proportion of IgA^+ bacteria in Ad.col – undiluted = 63%; 1:3 = 51%; 1:9 = 30%; 1:27 = 7.2%; G, red). On the contrary, Nb.col have shown the same anti-IgA profile that non-colonized (SPF) animals indicated by a reduced proportion of IgA-coated bacteria (Figure 5, F; proportion of IgA^+ bacteria in Nb.col – undiluted = 0.11%; 1:3 = 0.07%; 1:9 = 0.05%; 1:27 = 0.07%; G, blue; proportion of IgA^+ bacteria in SPF – undiluted = 0.06%; 1:3 = 0.05%; 1:9 = 0.05%; 1:27 = 0.04%; G, grey).

3.4. *Hh* distribution throughout the mouse gut

3.4.1. *Hh* detection in colonized mice by PCR

The differences seen between Ad.col and Nb.col mice with *Hh* led us to question how this pathobiont adapts to its host under these distinct challenges. Therefore, to get more insight about its localization and distribution across the mouse GI tract upon these contrasting colonization conditions we sampled 6 different regions of the mouse intestine: duodenum, jejunum, ileum, colon and rectum, depicted in Figure 3 (A); processed for DNA extraction afterwards. Moreover, because we had data suggesting that *Hh* could be crossing the intestinal barrier in mice colonized as adults, indicated by the presence of both IgG and IgM in their serum (data not shown), we decided to examine whether we could find it within different internal organs, namely the MLN, liver, GB and spleen (Figure 3, B) that were processed for DNA extraction.

For *Hh* detection we used *Hh*-specific 16S rRNA primers (PCR product size: 417 bp; Table 6.2; Appendix), whereas 18S rRNA primers (component of the small eukaryotic ribosomal subunit; PCR product size: 137 bp; Table 6.2; Appendix) was used as an internal control for amplification. Because all of our samples consisted essentially in mouse intestinal/organ tissue, we considered 18S rRNA a robust control for amplification and further a normalizer for the relative quantification of *Hh* load by qPCR.

Primarily, we sampled only different intestinal regions from B6 Nb.col animals (n=6) to test whether we could detect H*h* by PCR (Figure 6, A-G). We were able to it *Hh* consistently in the ileum, caecum and colon from all the animals tested (Figure 6, A-G; ile, cae, col). For the remaining intestinal regions, there was variation between the different animals (Figure 6, A-G; duo, jej, rec).

Identification of the niches occupied by *Hh* in the GI tract of healthy B6 mice in any age of colonization – adult vs neonate – was evaluated through quantification of *Hh* load by qPCR across the different intestinal regions and organs indicated above. Concomitantly with this question, a higher faecal load of *Hh* in immunodeficient – $Rag2^{-/-}$ – mice colonized as adults compared to B6 Ad.col mice (unpublished data) encouraged us to explore whether the absence of a full immune function involves advanced crossing of the intestinal epithelium. So, we collected the different intestinal regions and organs from $Rag2^{-/-}$ that were tested for *Hh* detection by PCR in a first step, and functioned as a quality control for *Hh* load quantification by qPCR that is shown ahead. Actually, *Hh* was detected within the MLN, rectum and spleen, but not within the liver from a $Rag2^{-/-}$ adult-colonized mouse (Figure 6, J; MLN, rec, spl, liv). However, it was not detected within the rectum from half of the newborn-colonized animals (Figure 6; A, B and D).

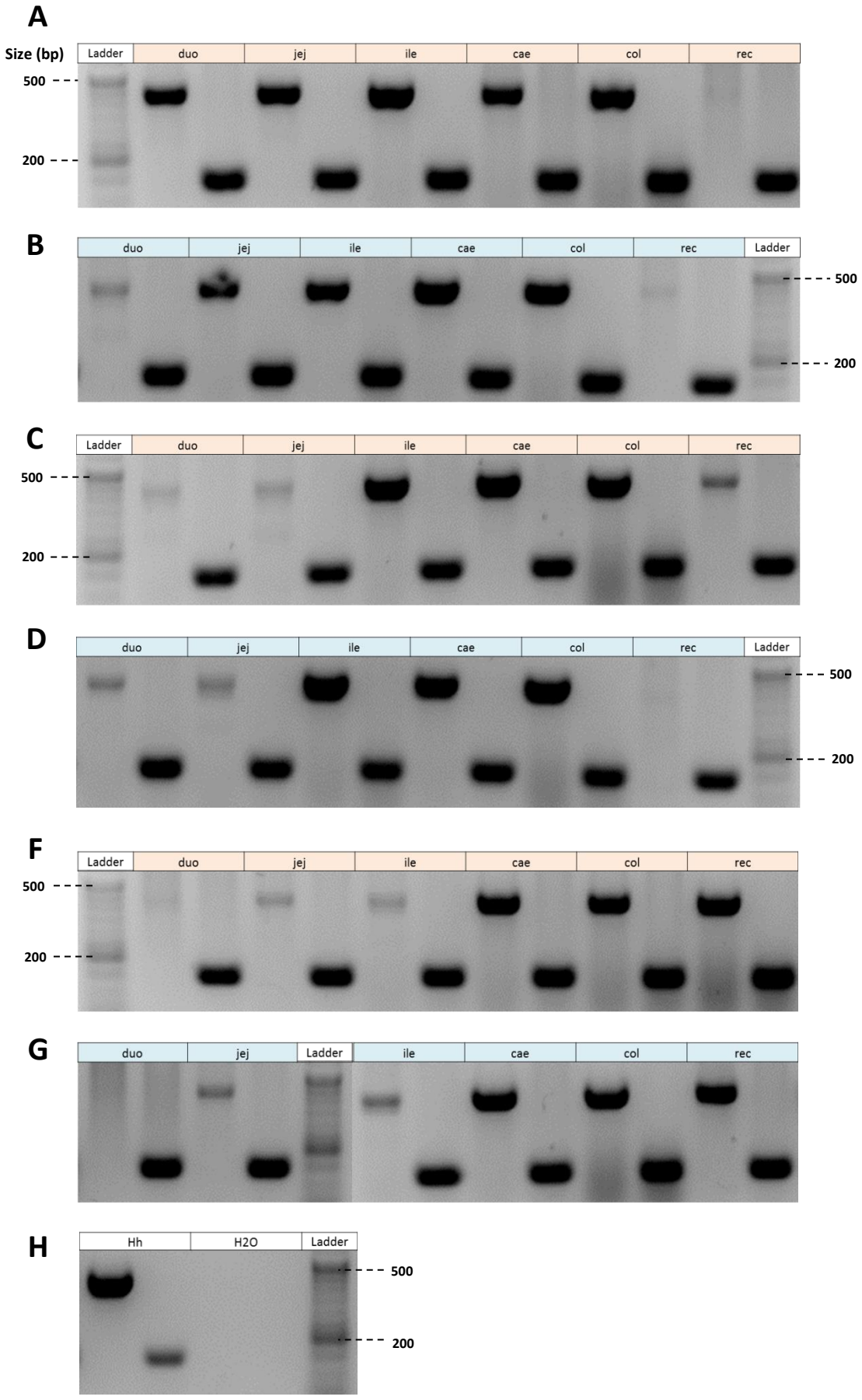
A
Size (bp)
Ladder
duo
jej
ile
cae
col
rec
500
200
B
duo
jej
ile
cae
col
rec
Ladder
500
200
C
Ladder
duo
jej
ile
cae
col
rec
500
200
D
duo
jej
ile
cae
col
rec
Ladder
500
200
F
Ladder
duo
jej
ile
cae
col
rec
500
200
G
duo
jej
Ladder
ile
cae
col
rec
H
Hh
H2O
Ladder
500
200

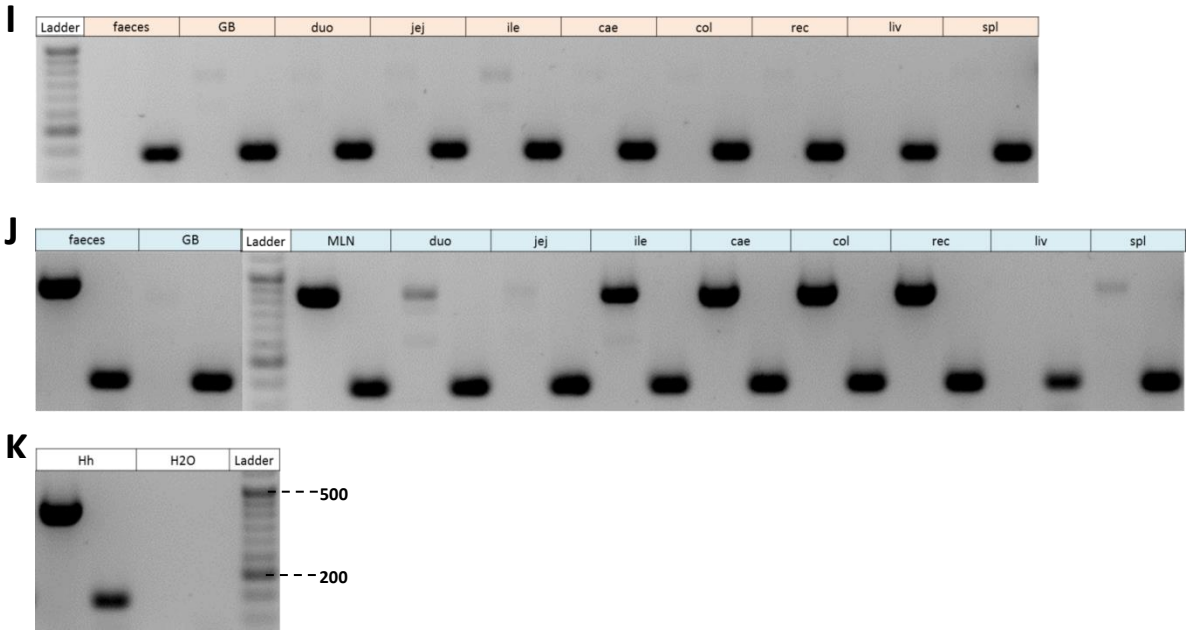

Figure 6. *Hh* detection in different mouse intestinal regions and organs by PCR. We used DNA from 6 regions of the mouse intestine – duodenum (duo), jejunum (jej), ileum (ile), caecum (cae), colon (col) and rectum (rec) – and organs – MLN, liver (liv), GB and spleen (spl) from B6 Nb.col (A-G), Rag2$^{-/-}$ SPF (I; n=1) and Rag2$^{-/-}$ Ad.col (J; n=1) mice. (A-G) *Hh* detection in the intestine from B6 Nb.col mice (n=6). Each gel represents a different mouse. Samples were tested for *Hh* 16S rRNA amplification. 18S rRNA (host DNA) was used as internal control. (H, K) DNA purified from cultured *Hh*: positive control for *Hh* 16S rRNA amplification; sterile water was used as a negative control (H2O). *Hh* detection in faeces, intestine and organs from B6 Rag2$^{-/-}$ SPF mice (I; no MLN from this mouse) and B6 Rag2$^{-/-}$ Ad.col mouse (J). PCR products were assessed in 0.5% Red Safe (1:4) 2% agarose gels. *Hh* 16S = 417 bp; 18S = 137 bp, analysed with DNA ladder (DNA Ladder VI, NZYTech). Gels were visualized in Gel Doc^{TM} XR.

As expected, *Hh* was not detected in any of the samples collected from a conventional SPF B6 Rag2$^{-/-}$ mouse (Figure 6, I) that had never been exposed to it. Conversely, it was found within faeces, MLN, duodenum, ileum, caecum, colon, rectum and spleen from a B6 Rag2$^{-/-}$ adult-colonized mouse (Figure 6, J).

3.4.2. *Hh* load quantification throughout the mouse GI tract by qPCR

As reported, besides the intestine other niches can be colonized within mammalian hosts such as the skin, upper and lower respiratory tract, among others [15]. Also, there is evidence that internal organs from immunocompetent hosts are usually maintained sterile, unlike the colon that is colonized by endogenous microbiota [15].

Given the results found by PCR, we performed a quantitative analysis on how *Hh* colonizes the mouse GI tract to identify its preferential niches within the intestinal microenvironment. Besides the contrast between Ad.col and Nb.col

B6 healthy mice, we have analysed Rag2$^{-/-}$ Ad.col mice as hosts lacking a full immune function. To evaluate total bacterial load, i.e., the

whole commensal bacteria community inside the gut, we estimated the ratio between total 16S copies (Eubacteria – Universal – 16S rRNA primers; Table 6.3, Appendix) and ng of host tissue DNA (Figure 7, A). To exclude bacterial contamination from the environment, we used non-template controls: qPCR mix for Eubacteria (total) 16S primers without DNA template, which normally contained ~10 total 16S copies vs 10^5 total 16S copies per well contained in our samples. To determine *Hh* load we used *Hh*-specific 16S rRNA primers (Table 6.3; Appendix): the number of *Hh*-specific 16S rRNA copies was normalized to the number of total 16S copies present within each sample; since all samples were retrieved from mouse tissue, to determine Hh load throughout the mouse GI tract the number of Hh-specific 16S rRNA copies was normalized to ng of host DNA (18S rRNA gene, Table 6.3; Appendix). Because we did not know how many copies of the 18S rRNA gene are present in host cells, we simply used 10 fold dilutions of the described DNA sample (Table 6.3; Appendix).

Within the proximal region of the SI – duodenum – we did not find differences between the 3 mouse groups that were analysed; in this region, we generally found 1-10 copies of Hh 16S per ng of host DNA [Figure 7, B – duodenum (median); D – duo (mean, SD)]. Similarly, we detected around 10 copies of Hh 16S per ng of host DNA in Rag2-/- Ad.col, compared to ~1 copy of Hh 16S in B6 Ad.col mice within the jejunum compartment [Figure 7, B; jejunum: 1 log fold difference between RG_adc vs WT_adc ($P<0.05$); median; D – jej, RG_adc vs WT_adc (mean, SD)].

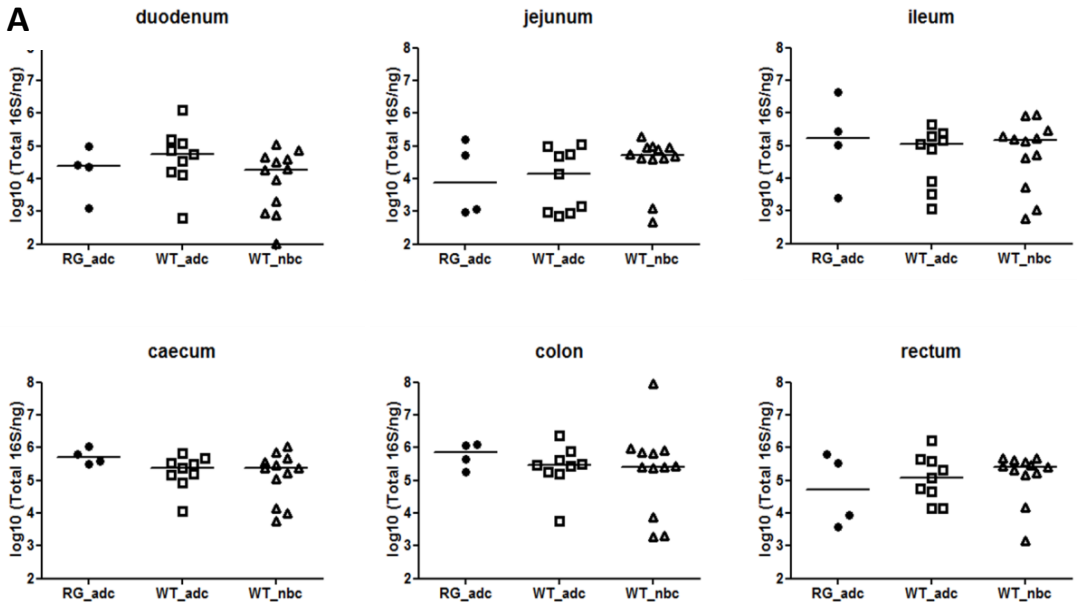

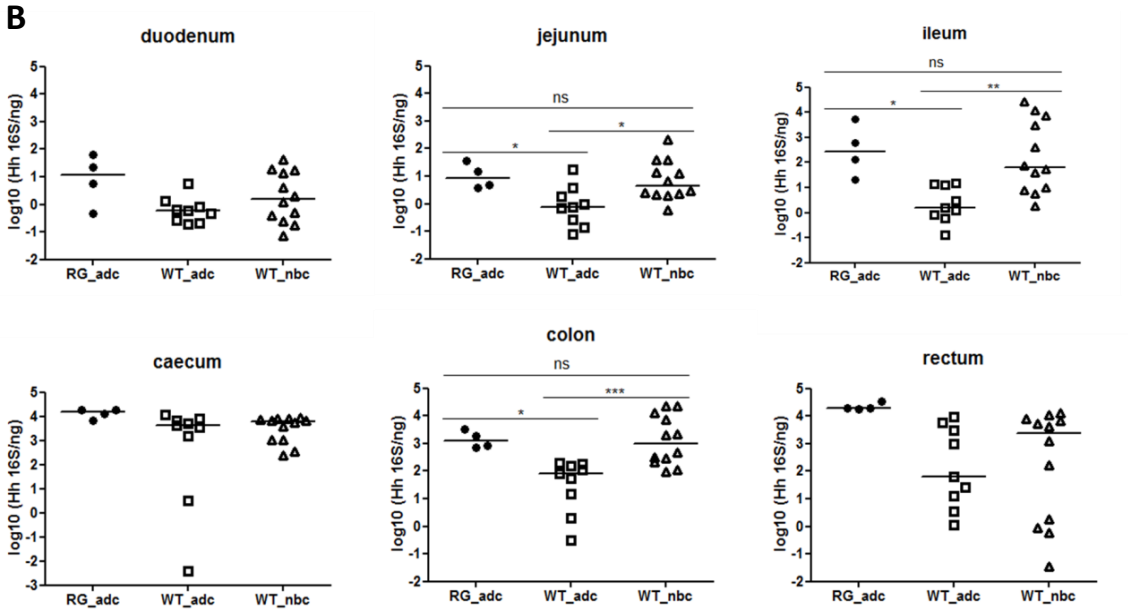
B
duodenum
jejunum
ileum
caecum
colon
rectum
log10 (Hh 16S/ng)
RG_adc
WT_adc
WT_nbc
ns
*
**
***

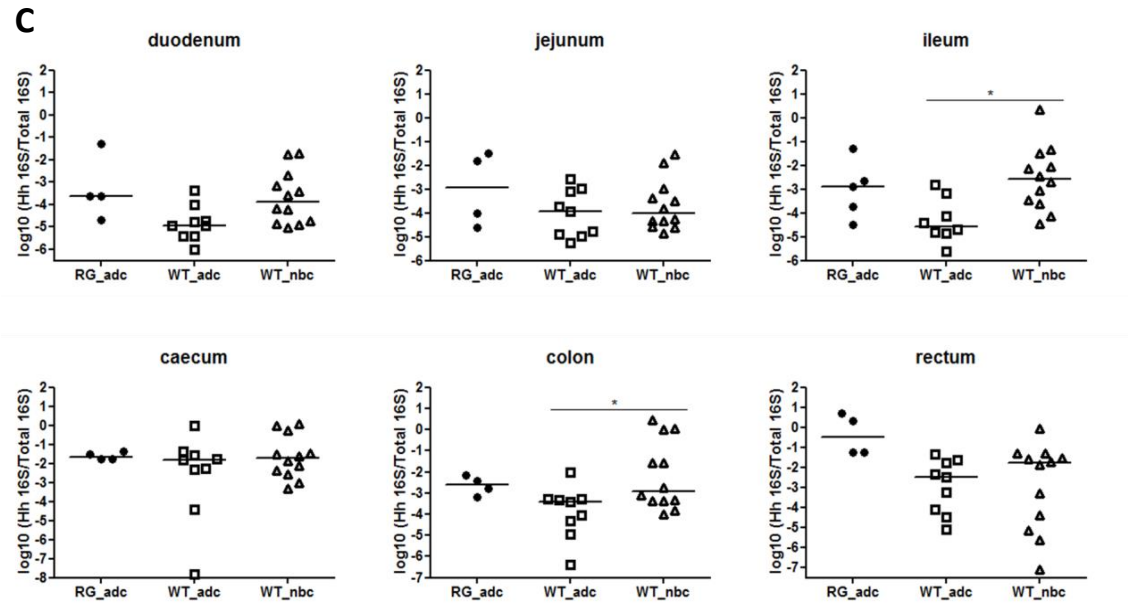
C
duodenum
jejunum
ileum
caecum
colon
rectum
log10 (Hh 16S/Total 16S)
RG_adc
WT_adc
WT_nbc
*

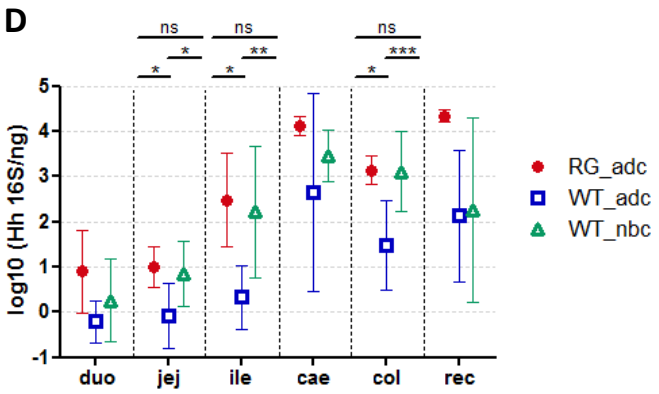
D
log10 (Hh 16S/ng)
duo
jej
ile
cae
col
rec
ns
*
**
***
RG_adc
WT_adc
WT_nbc

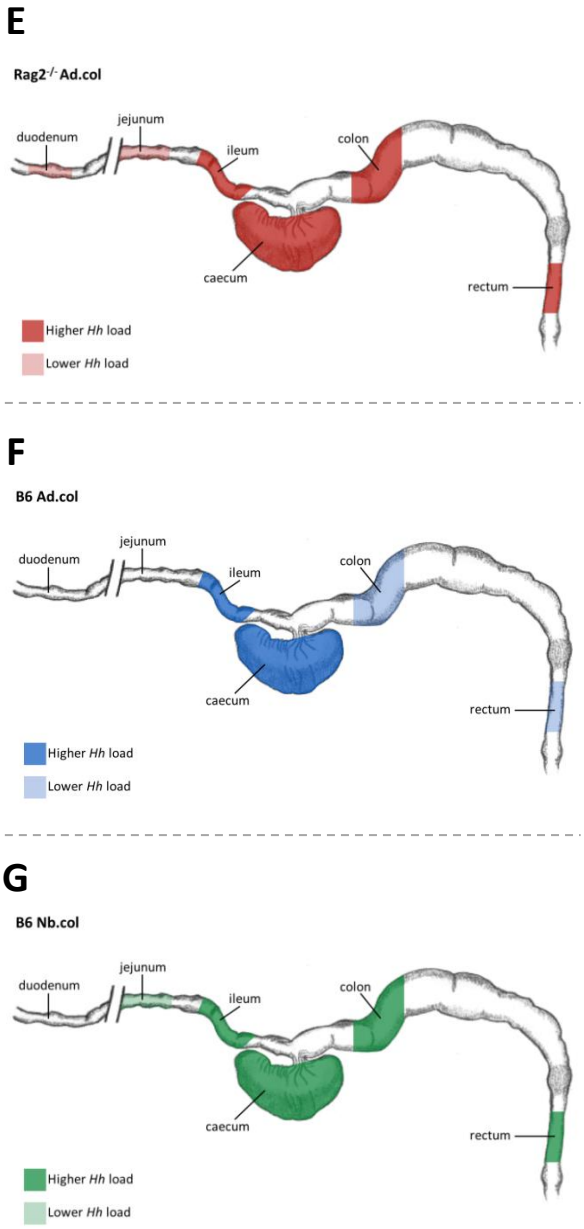

Figure 7. *Hh* distribution throughout the mouse GI tract.

Load in duodenum, jejunum, ileum, colon and rectum.

Ratio between total (Eubacteria) 16S copies normalized to ng of host DNA (A), *Hh*-specific 16S copies normalized to ng of host DNA (B), *Hh*-specific 16S copies normalized to total 16S copies (C). Rag2$^{-/-}$ Ad.col (**RG_adc,** n=4); B6 Ad.col (**WT_adc**, n=13); B6 Nb.col (**WT_nbc,** n=12).

(B) **jejunum**: RG_adc vs WT_adc (*P<0.05), WT_adc vs WT_nbc (*P<0.05); median. **ileum:** RG_adc vs WT_adc (*P<0.05), WT_adc vs WT_nbc (**P<0.01); median. **colon:** RG_adc vs WT_adc (*P<0.05), WT_adc vs WT_nbc (***P<0.001); median. (C) **ileum:** WT_adc vs WT_nbc (*P<0.05). **colon:** WT_adc vs WT_nbc (*P<0.05); median. Line in graphs A-C: median from each group. (D) *Hh* distribution profile throughout the GI tract between the 3 groups (*Hh*-specific 16S copies/ng host DNA ratio; mean, SD). Anatomical representation of the niches occupied within the gut from Rag2$^{-/-}$ Ad.col (E), Ad.col (F) and Nb.col (G) mice. One-way ANOVA and Tukey's Multiple Comparison (95% confidence interval) statistical tests. Graphs and data analysis done in GraphPad Prism software.

Hh load between B6 Ad.col and Nb.col mice was significantly different as well: animals challenged as newborns showed, roughly, a log fold higher in *Hh* burden [Figure 7, B; jejunum: WT_adc vs WT_nbc (P<0.05); median; D – jej, (mean, SD)].

Within the distal area of the SI – ileum – we detected a 2 log fold higher *Hh* load in Rag2$^{-/-}$ Ad.col compared to B6 Ad.col mice; like between B6 Ad.col and Nb.col mice [Figure 7, B; ileum: 2 log fold difference, RG_adc vs WT_adc (P<0.05); ileum: ~1.5 log fold difference, WT_adc vs WT_nbc (P<0.05); median;

D – ile, mean, SD]. Interestingly, a fairly high load of this microbe (10^3 copies of *Hh* 16S per ng of host DNA) was found within the colon from Rag2$^{-/-}$ Ad.col and B6 Nb.col mice [Figure 7, B; 1 log fold difference between RG_adc vs WT_adc ($P<0.05$) and WT_adc vs WT_nbc ($P<0.05$); RG_adc – D (ile; mean, SD), E; WT_nbc – D (ile; mean, SD), G].

Overall, a higher *Hh* load was seen within the caecum from all mice tested in relation to the other intestinal regions (Figure 7, B; caecum: 10^4 copies of *Hh* 16S per ng of host DNA, median; D – cae, mean, SD). Despite the quite high load detected within the rectum from Rag2$^{-/-}$ Ad.col mice, there were no major changes between the different animals that were analysed. Yet, a substantial variation within B6 Ad.col and Nb.col mice groups can be appreciated (consistent with what we have seen for *Hh* detection by PCR, particularly for Nb.col mice); whereas rectum samples from Rag2$^{-/-}$ Ad.col mice (n=4) showed a constant bacterial load (Figure 7, B; RG_adc, median; D – rec, mean,SD).

Within the 3 experimental mice groups all samples contained roughly the same amount of total bacteria load per ng of host DNA (Figure 7, A; median).

Amongst the entire intestinal bacterial community, *Hh* load is changed between B6 Ad.col and Nb.col ileum [Figure 7, C; ileum – WT_adc vs WT_nbc ($P<0.05$), median; D – ile (mean, SD)]. Within the ileum from B6 Nb.col the load of *Hh* was almost 2 log fold greater than in B6 Ad.col mice. Similarly, the colon from B6 Nb.col contained higher loads of *Hh* than B6 Ad.col mice [Figure 7, C; colon **–** WT_adc vs WT_nbc ($P<0.05$), median; D – col (mean, SD)].

3.5. *Hh* ability to traverse the intestinal epithelium

It is known that *Hh* has been originally isolated from the liver and colon of infected inbred strains of A/JCr mice and that it was associated to chronic active hepatitis and inflammatory bowel disease (Avenaud et al., 2003; Fox et al., 2011). After exploring the distribution of *Hh* across the mouse gut, we questioned whether it could penetrate the intestinal barrier in healthy B6 Ad.col and Nb.col mice, and in Rag2$^{-/-}$ Ad.col. Therefore, we collected the MLN, liver, GB and spleen from these animals, followed by quantification of *Hh* load by qPCR (Figure 9, A-C).

In Rag2$^{-/-}$ Ad.col MLN, we found a 3 log fold higher *Hh* load compared to either B6 Ad.col or Nb.col mice [Figure 8, B; ~1000 copies *Hh* 16S/ng host DNA in Rag2$^{-/-}$ Ad.col; RG_adc vs WT_adc, RG_adc vs WT_nbc ($P<0.05$); median]. In the MLN from Ad.col and Nb.col mice, quantification by qPCR revealed very low *Hh* burden (Figure 8, B; WT_adc and WT_nbc: ~1

copy of *Hh* 16S/ng host DNA; median). When we look at the load of total bacteria within MLN from Rag2$^{-/-}$ Ad.col mice, it is significantly higher compared to the other groups (Figure 8, A; 10^6 copies of *Hh* 16S/ng host DNA; median), although there is considerable variation within this group.

Though only 1-10 copies of *Hh* 16S were detected within the GB from Nb.col mice, this microbe was not detected within the GB from Ad.col mice [Figure 8, B; WT_adc vs WT_nbc (P<0.05); GB_{WT_adc} = ~0.1 copies of *Hh* 16S/ng host DNA; GB_{WT_nbc} = ~1-10 copies of *Hh* 16S/ng host DNA median]. Within the GB, no differences were found in *Hh* load between Rag2$^{-/-}$ Ad.col and B6 Nb.col mice (Figure 8, B; GB_{RG_adc} and GB_{WT_nbc} = ~1-10 copies of *Hh* 16S/ng host DNA; median).

We did not find significant differences in total bacteria load within the GB between the groups (Figure 8, A; 10^4-10^5 total 16S copies/ng of host DNA).

Higher *Hh* number was seen within the total bacteria contained in the MLN from Rag2$^{-/-}$ Ad.col mice, compared to the remaining groups (Figure 8, C; MLN: RG_adc vs WT_adc and RG_adc vs WT_nbc (P<0.05); median). In fact, we estimated that around only 0.1% of the total bacteria contained in Rag2$^{-/-}$ Ad.col MLN are *Hh* bacteria (Figure 8, C; MLN_{RG_adc} = 10^{-2}-10^{-3} *Hh* 16S copies per Total 16S copies; median). Whereas *Hh* was undetectable within bacteria contained in MLN from both B6 Ad.col Nb.col (Figure 8, C; MLN_{WT_adc} and MLN_{WT_nbc} = ~10^{-4}). We did not detect *Hh* 16S copies by qPCR amongst the total bacteria contained within the liver, GB and spleen from any of the groups tested (Figure 8, C; Liver, GB and Spleen from RG_adc, WT_adc and WT_nbc: globally ~10^{-4}; median).

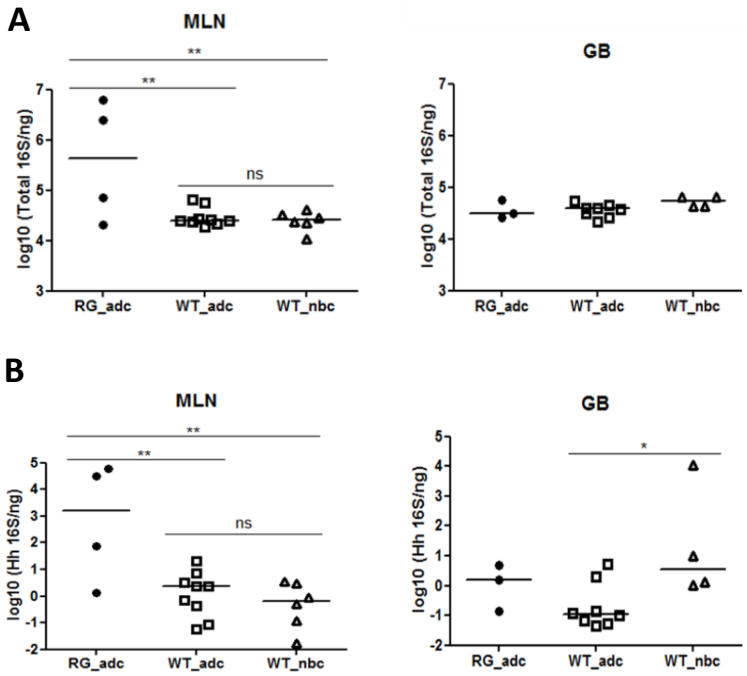

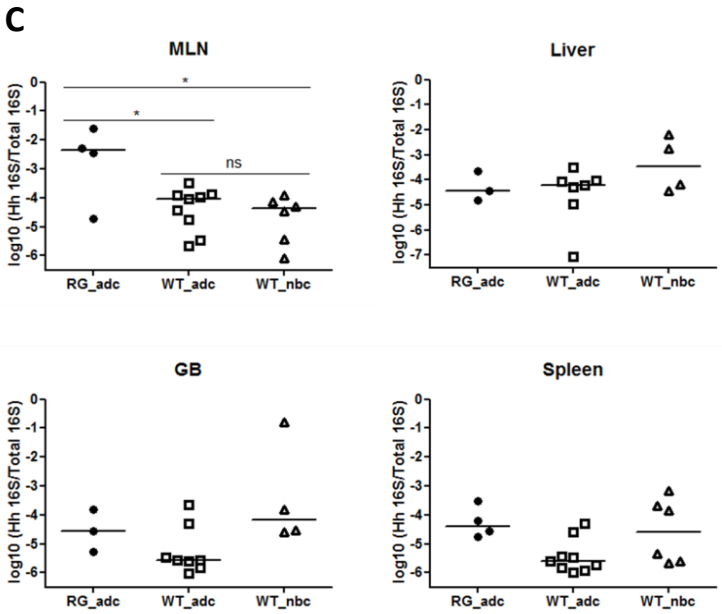

Figure 8. *Hh* ability to traverse the intestinal epithelium to colonize other organs is undetermined. *Hh* load quantification by qPCR within MLN, GB, liver and spleen. (A) Number of total 16S copies normalized to ng of host DNA. (B) Number of *Hh*-specific 16S copies normalized to ng of host DNA. (C) Number of *Hh*-specific 16S copies normalized to total 16S copies. **RG_adc** – $Rag2^{-/-}$ Ad.col (n=4), **WT_adc** – B6 Ad.col (n=13), **WT_nbc** – B6 Nb-col (n=12). (A) **MLN:** RG_adc vs WT_adc and RG_adc vs WT_nbc (**P<0.01). (B) **MLN:** RG_adc vs WT_nbc and WT_adc vs WT_nbc (**P<0.01). **GB:** WT_adc vs WT_nbc (*P<0.05). (C) **MLN:** RG_adc vs WT_adc and RG_adc vs WT_nbc (*P<0.05). One-way ANOVA and Tukey's Multiple Comparison (95% confidence interval) statistical tests. Line shown in each graph represents the median from each group. Graphs and data analysis executed on GraphPad Prism software.

3.6. Effect of *Hh* colonization on the progression of intestinal pathology

3.6.1. Experimentally-induced colitis in SPF, Ad.col and Nb.col mice

Our previous divergent results seen between B6 Ad.col and Nb.col led us to question whether their inflammatory profile is different when the intestinal epithelial barrier integrity is compromised and whether *Hh* colonization promotes progression of the inflammation response.

To understand whether *Hh* colonization is detrimental in the context of intestinal pathology we used the DSS-induced colitis model. We added 3% (w/v) DSS [25] to the drinking water of B6 SPF, Ad.col and Nb.col mice (n=5 per group) and weighed the animals at day 0, 3, and 5; from this point on, the weight was recorded daily until animals recovered the initial weight. DSS was removed at day 8, such that animals could recover from inflammation.

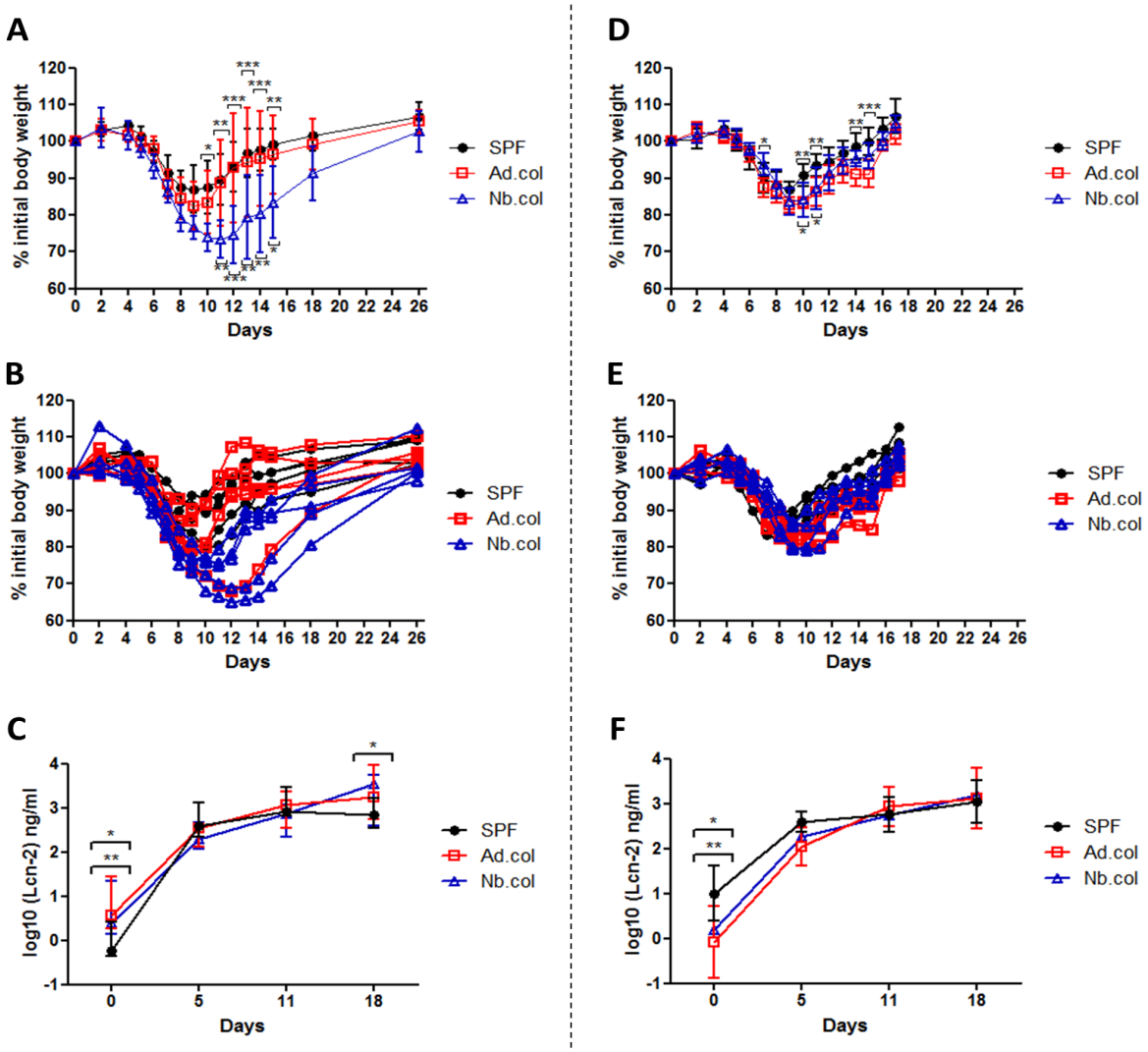

Figure 9. Effect of *Hh* colonization on the progression of intestinal inflammation. B6 SPF, Ad.col and Nb.col mice were given 3% (w/v) DSS (n=5 per group). (A, C) Weight throughout the experiment (mean, SD).

(B, E) Weight throughout the experiment (each replicate). (C, F) Faecal Lcn-2 levels at days 0, 5, 11 and 18 (ELISA). The results shown correspond to two independent experiments (A-C; D-F).

(A) SPF vs Ad.col: ns; SPF vs Nb.col: day 10, *P<0.05; day 11, **P<0.01; days 12, 13, 14, ***P<0.001; day 15, *P<0.01. Ad.col vs Nb.col: day 11, **P<0.01; day 12, ***P<0.001; days 13, 14, **P<0.01; day 15, *P<0.05.

(C) SPF vs Ad.col: day 0, **P<0.01; day 18, *P<0.05. SPF vs Nb.col: day 0, *P<0.05. Ad.col vs Nb.col: ns. (D) SPF vs Ad.col: days 10, 11, 14, **P<0.01; day 15, ***P<0.001. SPF vs Nb.col: days 10, 11, **P<0.01. Ad.col vs Nb.col: day 7, *P<0.05.

(F) SPF vs Ad.col: day 0, **P<0.01. SPF vs Nb.col: day 0, *P<0.05. Ad.col vs Nb.col: ns. Two-way ANOVA and Bonferroni (post-test) were used as statistical tests. Graph and data analysis executed on GraphPad Prism software.

Besides the body weight development, severity of the intestinal inflammation was also assessed by measurement of lipocalin (Lcn-2) levels in faeces by ELISA [3] at days 0, 5, 11 and 18.

As expected, a decrease in body weight starting around day 4 was observed in both experiments (Figure 9, A and D). Within the first DSS experiment (Figure 9, A-C), body weight was recorded until day 26 to ensure recovery from all experimental groups. In this case, a constant weight reduction until day 9 was seen in all groups (Figure 9, A).

From this time point onwards, however, some of the Nb.col mice had a significantly higher weight loss over SPF and Ad.col mice [Figure 9, B – Nb.col, blue; A –SPF vs Nb.col: day 10 ($P<0.05$); day 11 ($P<0.01$); days 12, 13, 14 ($P<0.001$); day 15 ($P<0.01$). Ad.col vs Nb.col: day 11 ($P<0.01$); day 12 ($P<0.001$); days 13, 14 ($P<0.01$); day 15 ($P<0.05$); mean, SD] accounting for the large variation seen in within this group (Figure 9, A – Nb.col, blue). Nevertheless, all animals started to gain weight after DSS removal around day 12-13, recovering the initial weight ultimately (Figure 9, A; 100% initial body weight). In the second experiment, similar differences in weight were found between the groups: at day 10, Ad.col weight was lower than Nb.col mice; at days 10, 11 and14, and significantly at day 15, Ad.col showed a lower weight reduction than SPF mice; at days 10 and 11, Nb.col mice showed a slightly higher weight reduction than SPF [Figure 9, D – SPF vs Ad.col: days 10, 11, 14, ($P<0.01$); day 15 ($P<0.001$). SPF vs Nb.col: days 10, 11 ($P<0.01$). Ad.col vs Nb.col: day 7 ($P<0.05$); mean, SD].

Faecal Lcn-2 levels (ELISA) revealed differences between the groups before induction of intestinal inflammation in both experiments and at day 18 within the first experiment [Figure 9, C – SPF vs Ad.col: day 0 ($P<0.01$); day 18 ($P<0.05$). SPF vs Nb.col: day 0, ($P<0.05$). Ad.col vs Nb.col: ns; mean, SD] but not within days 5 and 11. Within both experiments, high levels of faecal Lcn-2 in all groups were still detected at day 18 (Figure 9, C and F; 3 log fold difference between days 0 and 18, for SPF and Ad.col and Nb.col).

4. DISCUSSION

The framework of this study was important not only to understand the mechanisms underlying host tolerance to commensal bacteria, but also to investigate the effect of commensals under intestinal disease. Here, we looked at a host-microbe relationship between mice and *Hh*.

To understand whether *Hh* tolerogenic potential is dependent on the presence of a complex microbiota, we performed monocolonization in B6 GF mice and measured the levels of faecal *Hh*-specific IgA. Like in SPF Ad.col mice (unpublished data), a strong *Hh*-specific IgA response was seen in Ad.mcol, (Figure 4, A and B; Ad.mcol). In contrast, in Nb.mcol animals we did not detect anti-*H. hepaticus* IgA (Figure, 4 A and B; Nb.mcol). This *Hh*-specific IgA profile similar to SPF animals suggests that the tolerant response elicited *Hh* is microbiota-independent, i.e., its tolerogenic potential induced when animals are colonized as newborn does not require the presence of other intestinal bacteria.

Although it is still uncertain whether IgA restricts growth of commensal bacteria or whether it confines their spread from the intestinal compartment by coating their surface; yet, it is estimated that more than 70% of total-body Ig synthesis consists in IgA[13]. Total IgA titre detected in faeces from Ad.mcol was not different from Nb.mcol (Figure 4, C; Ad.mcol, Nb.mcol = ~1 µg/ml of faeces; median). Since monocolonized animals had never been exposed to commensal bacteria before, lower total IgA titre detected in faeces from Ad.mcol mice is expected. Because their intestinal mucosa was not adapted to commensal bacteria, it is likely that IgA production was stimulated only after the challenge with *Hh*. Likewise, if we had tried to perform a bicolonization experiment, i.e., challenge with 2 different bacterial strains, we would find a total IgA titre probably in between the adult-colonization and adult-monocolonization titres.

Later, we demonstrated how IgA interacts with *Hh* bacterial cells physiologically: it binds specifically to *Hh* surface. IgA binding directly to *Hh* surface was ascertained by incubation of faecal extracts from different experimental groups – SPF, Ad.col, Nb.col – with *Hh* bacteria grown in culture, and analysed by flow cytometric. While in faeces from Ad.col mice, the proportion of IgA^+ *Hh* can get up around 60%, in faeces from either SPF or Nb.col mice this bacterial population is represented in less than 1% (Figure 5, F; undiluted – first row of plots).

We were able to detect the IgA^+ population even under serial dilutions of faecal extract from Ad.col animals, showing that a substantial concentration of *Hh*-specific IgA must be produced in this robust response (Figure 5, F; G – red). Faecal extract from Ad.col under a 1:27 dilution factor exhibited a significantly higher proportion of IgA^+ bacteria than any of the undiluted faecal extracts from either SPF or Nb.col mice (Figure 5, F; $IgA^+_{\text{Ad.col (1:27)}} = 7.2\%$ vs $IgA^+_{\text{Nb.col (undiluted)}}$,

$IgA^{+}_{SPF\ (undiluted)}$ < 1%). Like SPF mice, Nb.col exhibited a very reduced proportion of IgA^{+} bacteria [Figure 5, F; G – $IgA^{+}_{Nb.col}$ (blue), IgA^{+}_{SPF} (grey)]. This is a consequence of the *Hh*-induced tolerant response upon neonatal-colonization, which corroborates previous data obtained by our group by ELISA (unpublished data).

Incubation with bacteria grown in culture rendered the possibility to preserve bacterial cell wall structure and integrity reproducing the interaction at the physiological level between the host (Ad.col mice) immune system – IgA – and intact bacterial cells; *Hh* structural properties were presumably undisturbed because bacterial colonies were scraped from growth plates and suspended directly in PBS, in order to estimate the CFU. Conversely, for detection of *Hh*-specific IgA by ELISA, plates are coated with *Hh* lysed bacteria, in which these structural properties are implicitly compromised.

Thus, through faecal IgA flow cytometry we were able to demonstrate that the Ig produced specifically against *Hh* binds directly to its surface using a technique that had never been performed in the lab before. Moreover, we conclude that the assay described above is a good model for what actually happens *in vivo*, when *Hh*-specific IgA antibodies encounter a bacterial cell: the affinity of IgA to *Hh* antigens must promote the binding and, consequently, *Hh* is coated with IgA in the intestinal lumen; as a result, *Hh* is prevented from crossing the epithelium.

Contrasting results seen between B6 Ad.col and Nb.col mice increased our curiosity about how this pathobiont colonizes the host under these distinct challenges. Therefore, we examined the distribution of *Hh* across the mouse GI tract upon these opposite colonization conditions.

The proximal SI – which includes the duodenum and jejunum in our setting – is the region where the mucus layer is less protective (Maynard et al., 2012); nevertheless, it was the region where we detected the lowest loads of *Hh* [Figure 7, B; duodenum, jejunum = 0-10 copies of *Hh* 16S/ng host DNA (median); D – duo, jej (mean, SD)]. Because the SI has an intrinsic digestive function and strong peristaltic movements, it leads to clearance of material from the luminal content also comprising commensals and other microbes [14, 29]. Moreover, it is an acidic and salt containing environment, because acid and bile salts are conveyed from the stomach and gallbladder, respectively. Together, these contents have an anti-microbial effect, resulting in lower bacterial loads in the proximal SI [14]. Additionally, as RegIIIγ selectively targets Gram-positive bacteria [30, 14] unlike *Helicobacter*, which is a genus of Gram-negative bacteria, *Hh* is not affected by this antimicrobial protein.

The intestinal mucus layer is thicker and continuous especially within the LI, but also in distal SI. It is documented that the highest microbial density populates the distal ileum and colon (10^8 and 10^{10}-10^{12} microbes per gram, respectively)

[12, 14]. Within the distal area of the SI – ileum – we detected a 2 log fold higher *Hh* load in Rag2$^{-/-}$ Ad.col compared to B6 Ad.col mice; like between B6 Ad.col and Nb.col mice [Figure 7, A; ileum – 2 log fold difference, RG_adc vs WT_adc ($P<0.05$); ~1.5 log fold difference, WT_adc vs WT_nbc ($P<0.01$), median; D (ile), mean, SD; Rag2$^{-/-}$ Ad.col (E), Ad.col (F), Nb.col (G)]. Interestingly, a fairly high load of this microbe (10^3 copies of *Hh* 16S/ng of host DNA) was found within the colon from Rag2$^{-/-}$ Ad.col and B6 Nb.col mice [Figure 7, B; colon – 1 log fold difference between RG_adc vs WT_adc ($P<0.05$) and WT_adc vs WT_nbc ($P<0.001$), median; D (col), mean, SD; Rag2$^{-/-}$ Ad.col (E), Nb.col (G)]. Moreover, a study that first described *Hh* revealed active motility due to a single flagellum at one or each edges of the bacteria, emphasizing that the flagella may be important for colonization of mucus[7] (which is thicker in the colon).

We generally found a higher *Hh* load within the caecum from all mice tested in relation to the other intestinal regions [Figure 7, B; caecum = 10^4 copies of *Hh* 16S/ng of host DNA, median; D (cae), mean, SD; Rag2$^{-/-}$ Ad.col (E), Ad.col (F), Nb.col (G)]. No major changes were seen between the different animals that were analysed regarding the rectum; nevertheless, we detected quite high load within the rectum from Rag2$^{-/-}$ Ad.col mice. Yet, a substantial variation within the Nb.col and Ad.col mice groups can be appreciated (consistent with what we have seen for *Hh* detection by PCR, particularly for Nb.cold mice); whereas rectum samples from Rag2$^{-/-}$ Ad.col mice (n=4) showed a constant bacterial load [Figure 7, B; rectum$_{RG_adc}$ = 10^4 copies of *Hh* 16S/ng of host DNA, median; D (cae), mean, SD; Rag2$^{-/-}$ Ad.col (E), Ad.col (F), Nb.col (G)].

Because *Hh* is microaerophilic, perhaps it has evolved to adapt to mucus-rich intestinal regions – ileum and colon – unlike the lower LI – rectum –, in which there must be higher oxygen content. This suggests that the lower part of the mouse GI tract might not be an advantageous microenvironmental niche for *Hh*, since it shows variation associated to the time of colonization and presence of the adaptive immune function.

A robust anti-*Hh* IgA immune response can explain the lower *Hh* burden throughout the GI tract from B6 Ad.col animals.

Actually, no significant differences were found between Rag2$^{-/-}$ Ad.col and B6 Nb.col mice, where this IgA response is not produced. Previous data from our group, showed higher faecal *Hh* burden in Rag2$^{-/-}$ than in B6 both colonized as adults (unpublished data). The absence of lymphocytes – lack of anti-*Hh* IgA and CD25$^+$ regulatory T cells – in Rag2$^{-/-}$ Ad.col mice leads to higher *Hh* loads in these animals. On the other hand, the long-lasting tolerant response induced when animals are challenged with *Hh* as newborns elucidates the increase of *Hh* number in these mice. When *Hh* is present at an early stage of life, the adaptive immunity promotes a mutualistic relationship with *Hh* rather than a defence one.

The entire bacterial community residing in the intestine did not differ throughout the intestinal regions analysed, within the 3 mice groups.

All samples contained roughly the same amount of total bacteria load per ng of host DNA (Figure 7, A; ~10^4-10^6 total 16S copies/ng of host DNA).

Within the ileum from B6 Nb.col the number of *Hh* 16S copies within the total bacteria contained in this region was almost 2 log fold greater than in B6 Ad.col mice (Figure 8, C – $ileum_{WT\_nbc}$: 1 in every 1000 bacteria is *Hh*; WT_adc vs WT_nbc ($P<0.05$); median). Similarly, the colon from B6 Nb.col contained higher loads of *Hh* than B6 Ad.col mice (Figure 8, C – $colon_{WT\_nbc}$: 1 in every 1000 bacteria is *Hh*; WT_adc vs WT_nbc ($P<0.05$); median). The differences between adult- and newborn-colonization found in these regions of the GI tract corroborate what had been seen for *Hh* load quantification in faeces before in the lab (*Hh* faecal load estimated by the ratio between *Hh* 16S/Total 16S is higher Nb.col mice; unpublished data).

Interestingly, under no circumstances we found statistically significant differences between $Rag2^{-/-}$ Ad.col and B6 Nb.col mice throughout the GI tract (Figure 8, A-C; D – RG_adc vs WT_nbc). This observation suggests that *Hh* uses a similar mechanism of adaptation in the gut of mice that have been colonized as neonates – no production of *Hh* specific-IgA – and in mice that lack a full immune function. When we estimated *Hh* load in different internal organs by qPCR, *Hh* traverse to colonize other organs remained undetermined. Although a 3 log fold higher was estimated within MLN from $Rag2^{-/-}$ Ad.col mice colonized as adults compared to the other groups (Figure 9, B; MLN: 10^3 vs 10^0 copies of *Hh* 16S per ng of host DNA, respectively), liver and spleen from all groups analysed (Figure 9, C; Liver, Spleen). Correspondingly, *Hh* was not detected by PCR within the liver from A/JCr and B6 mice experimentally colonized [36].

GB from Nb.col and $Rag2^{-/-}$ Ad.col mice had positive results of qPCR analysis for *Hh* 16S rRNA, but not in GB samples from the other groups (Figure 9, B; $GB_{Nb.col}$ – ~10 copies of *Hh* 16S/ng of host DNA; $GB_{Rag2^{-/-}\ Ad.col}$ = 1 copy of *Hh* 16S/ng of host DNA; median), suggesting that there could be penetration of the intestinal epithelium in both $Rag2^{-/-}$ Ad.col and Nb.col mice.

It was reported that when B6 mice are submitted to ig colonization with *Enterobacter cloacae*, intestinal dentritic cells (DCs) sample these live bacteria and then can circulate into the MLN [13]. Interestingly, after ig challenge, *E. cloacae* could be retrieved from MLN but not from spleen or other tissues [13]. Conversely, culture of spleens from *Salmonella typhimurium*-colonized mice resulted in detectable growth of these bacteria, indicating penetration of the intestinal epithelium. It was revealed further that cultured DCs and macrophages sorted from MLN from these mice contained *Salmonella* [13]. So, it was established that commensal but not pathogenic bacteria, are killed by

macrophages and only survive inside intestinal DCs at lower number, thus, being confined to the intestinal immune compartment rather than spreading to the systemic one.

Thus, *Hh* load that we estimated in MLN might account for bacteria residing inside intestinal DCs that entered the MLN. Indeed, *Hh* load in liver and spleen from Rag2$^{-/-}$ Ad.col mice was undetectable by qPCR, which was also the case for both Ad.col and Nb.col mice (Figure 9, C; Liver and Spleen).

Since the liver is a big size organ, if we had used the same processing protocol for DNA extraction that was used for the other samples, quantification of *Hh* load by qPCR would be impaired. This is because there would be much more host cells rather than bacterial cells; therefore, to increase access to bacteria contained within the liver, we decided to shatter the entire organ in PBS using a nylon mesh transferring the whole volume into a tube, followed by centrifugation. In this situation, because bacterial cells are smaller than mammalian cells, we collected the supernatant containing the bacteria from which we extracted DNA. This treatment was also used for the spleen. Possibly, it was not the most effective procedure to sample organs for load quantification by qPCR. Alternatively, assessment of the bacterial load by culture and subsequent CFU counting would be a convenient experiment to complement our results; so it would be clear whether we can detect *Hh* grown in culture especially from the liver and spleen.

On the other hand, Kupffer cells, which reside in the liver, phagocytize commensal bacteria from blood, thus, being responsible for their clearance [2]. As the liver receives venous blood from the intestine, it was described as a “firewall” by clearance of commensal bacteria that enter the bloodstream [2]. As documented by colonization ig with *E. coli* of healthy WT mice, live bacteria were detected in MLN but not in the liver. However, bacterial products were detected within hepatic tissues, providing evidence that entrance of live microbes into the MLN is independent from their traffic into the liver or the spleen from a healthy animal [2]. This proved that the liver provides a secondary firewall for bacteria that encounter blood vessels during intestinal pathology or upon penetration of the epithelial layer.

When we assessed the load of *Hh* between Ad.col and Nb.col mice, higher number of *Hh* was retrieved in the GI tract and GB from Nb.col mice but not within the liver and spleen (Figure 6, B and C, respectively). It is known that the B6 mouse strain is less prone to the development of *Hh*-linked disease. As fascinating as it is, it seems that there is a complex “arms race” between *Hh* infection and host defence. Not long after *Hh* has been originally isolated (90s), production of a *Hh* virulence factor that induces cell cycle arrest leading to apoptosis on one side, and genes that confer resistance to *Hh* in the mouse on the other side were documented [44]. As reported within this study, host genetic

factors influence resistance/susceptibility to *Hh;* besides the action of the intestinal mucosa, systemic immunity and changed sensitivity to *Hh* cytotoxins are operating mechanisms in this context. Among other factors, presence of specific immune cells in the liver or quantitative expression of T helper cell cytokines stimulating bacteria elimination by macrophages were advocated as possible mediators of the commensal-like response to *Hh* [44].

Our qPCR analysis of *Hh* load was not enough to determine whether *Hh* traffics to other organs. Nevertheless, it allowed us to find which microenvironmental niches are occupied by this pathobiont within the mouse GI tract. Still, because B6 Ad.col and Nb.col differ in their response to *Hh* we questioned whether their inflammatory profile is different if the integrity of the intestinal barrier is compromised.

Two independent experiments showed relative reproducibility (Figure 10). As expected, a decrease in body weight starting around day 4 was observed in both experiments (Figure 10, A and D), as seen by others [3].

Within the first DSS experiment (Figure 10, A-C), body weight was recorded until day 26 to ensure recovery from all experimental groups. In the course of this experiment, a constant weight reduction until day 11 was seen in all groups (Figure 10, A). From this time point onwards, however, some of the Nb.col mice had a significantly higher weight loss over SPF and Ad.col mice (Figure 10, B; Nb.col, blue) accounting for the large variation seen in Figure 10 – A within this group. Nevertheless, all animals started to gain weight after DSS removal around day 12-13, recovering the initial weight ultimately (Figure 10, A; 100% initial body weight). In the second experiment, some differences in weight were also appreciated between the groups from day 10 onwards, though at fewer time points (Figure 10, D).

Faecal Lcn-2 levels by ELISA showed no correlation between body weight recovery and faecal levels of this protein. Indeed, we have seen differences between the groups at steady state in both experiments, and at day 18 within the first experiment (Figure 7, C – SPF vs Ad.col: day 0 ($P<0.01$); day 18 ($P<0.05$); SPF vs Nb.col, ($P<0.05$); F – SPF vs Ad.col: day 0 ($P<0.01$); SPF vs Nb.col ($P<0.05$); mean, SD). Within both experiments, we still detected high levels of faecal Lcn-2 in all groups at day 18 (Figure 7, C and F; 3 log fold difference between days 0 and 18, for SPF and Ad.col and Nb.col).

Because animals were given regular water at day 8, we were not expecting to see such high amount of this protein at this time point. In another study, in which 1.5% (w/v) DSS solution was used to model colitis in mice for 7 days (n=5; DSS removal at day 7), faecal Lcn-2 levels started to decrease at day 15 [3]. In our study, although all animals have recovered their initial body weight (Figure 7, A and D), a 3% (w/v) DSS solution was used to induce inflammation in mice, which might have caused a delay in the mucosal healing process. To

ascertain whether faecal Lcn-2 levels decreased at some point after the removal of DSS in our mice, we should have collected faecal samples at the time animals were euthanized to collect blood for serum preparation. Moreover, we could have seen whether the tolerant response induced by *Hh* in Nb.col mice is maintained under intestinal inflammation. Since we have faecal and serum samples collected throughout the experiment, we could assess whether the levels of faecal and serum IgA are not detected in Nb.col mice in this circumstances.

Furthermore, it would be interesting to perform qPCR analysis and culture from the different intestinal areas and internal organs sampled from mice that were experimentally induced with colitis. As their intestinal epithelial barrier integrity is compromised, *Hh* traffic out of the intestine would be more likely. Unlike healthy mice colonized with *Hh* which have an impermeable epithelium that is fully functional, the DSS treatment has a damaging effect on this physical barrier. As a result, the non-continuous intestinal epithelial structure cannot confine *Hh* that can reach the blood stream and can colonize other organs.

Having a deeper perception of the interactions between hosts and their commensals provides insight about how tolerance to commensal bacteria is regulated and how it can be maintained, as well as colonization resistance to pathogens. In this sense, evolution of long-lasting neonatal tolerance to *Hh* in mice possibly arisen to prevent pathogen infection during early life, although the mechanisms underlying it require further investigation. Immune unresponsiveness to *Hh* evokes deliberate maintenance of this bacterial species, being tolerized by the host owing to early lifetime exposure.

Because *Hh* has been described as counterpart of the human *H. pylori*, known to induce gastritis in humans, and it has been extensively used to model diseases such as chronic hepatitis, hepatic cancer and, lately IBD, it seemed important to study the impact of *Hh* on intestinal pathology, which is still not completely understood.

5. REFERENCES

1. Avenaud, P. *et al.* Natural History of Helicobacter hepaticus Infection in Conventional A / J Mice , with Special Reference to Liver Involvement Natural History of Helicobacter hepaticus Infection in Conventional A / J Mice , with Special Reference to Liver Involvement. *Society* **71,** 3667–3672 (2003).

2. Balmer, M. L. *et al.* The liver may act as a firewall mediating mutualism between the host and its gut commensal microbiota. *Sci. Transl. Med.* **6,** 237ra66 (2014).

3. Chassaing, B. *et al.* Fecal Lipocalin 2, a Sensitive and Broadly Dynamic Non-Invasive Biomarker for Intestinal Inflammation. *PLoS One* **7,** 3–10 (2012).

4. Cheesman, S. E. & Guillemin, K. We know you are in there: Conversing with the indigenous gut microbiota. *Res. Microbiol.* **158,** 2–9 (2007).

5. Cong, Y., Feng, T., Fujihashi, K., Schoeb, T. R. & Elson, C. O. A dominant, coordinated T regulatory cell-IgA response to the intestinal microbiota. *Proc. Natl. Acad. Sci. U. S. A.* **106,** 19256–19261 (2009).

6. Fox, J. G., Ge, Z., Whary, M. T., Erdman, S. E. & Horwitz, B. H. *Helicobacter hepaticus* infection in mice: models for understanding lower bowel inflammation and cancer. *Mucosal Immunol.* **4,** 22–30 (2011).

7. Fox, J. G. *et al. Helicobacter hepaticus* sp. nov., a microaerophilic bacterium isolated from livers and intestinal mucosal scrapings from mice. *J. Clin. Microbiol.* **32,** 1238–1245 (1994).

8. Hand, T. W. *et al.* Acute Gastrointestinal Infection Induces Long-Lived Microbiota-Specific T Cell Responses. *Science* **337,** 1553–1556 (2012).

9. Hooper, L. V & Gordon, J. I. Commensal host-bacterial relationships in the gut. *Science* **292,** 1115–1118 (2001).

10. Kamada, N., Chen, G. Y., Inohara N., Núñez G., *Nat Immunol.* **14,** 685–690 (2013).

11. Kawamoto, S. *et al.* Foxp3+ T Cells Regulate Immunoglobulin A Selection and Facilitate Diversification of Bacterial Species Responsible for Immune Homeostasis. *Immunity* **41,** 152–165 (2014).

12. Ley, R. E., Peterson, D. a. & Gordon, J. I. Ecological and evolutionary forces shaping microbial diversity in the human intestine. *Cell* **124,** 837–848 (2006).

13. Macpherson, A. J. & Uhr, T. Induction of protective IgA by intestinal dendritic cells carrying commensal bacteria. *Science* **303,** 1662–1665 (2004).

14. Maynard, C. L., Elson, C. O., Hatton, R. D. & Weaver, C. T. Reciprocal interactions of the intestinal microbiota and immune system. *Nature* **489,** 231–241 (2012).

15. Medzhitov, R. Recognition of microorganisms and activation of the immune response. *Nature* **449,** 819–826 (2007).

16. Mirpuri, J. *et al.* Proteobacteria-specific IgA regulates maturation of the intestinal microbiota. *Gut Microb.* **5**:1, 1–12 (2014).

17. Molloy, M. J., Bouladoux, N. & Belkaid, Y. Intestinal microbiota: Shaping local and systemic immune responses. *Semin. Immunol.* **24,** 58–66 (2012).

18. Molloy, M. J. *et al.* Intraluminal containment of commensal outgrowth in the gut during infection-induced dysbiosis. *Cell Host Microbe* **14,** 318–328 (2013).

19. Muniz, L. R., Knosp, C. & Yeretssian, G. Intestinal antimicrobial peptides during homeostasis, infection, and disease. *Front. Immunol.* **3,** 1–13 (2012).

20. Round, J. L. & Mazmanian, S. K. The gut microbiota shapes intestinal immune responses during health and disease. *Nat. Rev. Immunol.* **9,** 313–323 (2009).

21. Saleh, M. & Trinchieri, G. Innate immune mechanisms of colitis and colitis-associated colorectal cancer. *Nat. Rev. Immunol.* **11,** 9–20 (2011).

22. Slack, E. *et al.* Innate and adaptive immunity cooperate flexibly to maintain host-microbiota mutualism. *Science* **325,** 617–620 (2009).

23. Valentini, M. *et al.* Immunomodulation by Gut Microbiota: Role of Toll-Like Receptor Expressed by T Cells. *J. Immunol. Res.* **2014,** 1–8 (2014).

24. Wei, M. *et al.* Mice carrying a knock-in mutation of Aicda resulting in a defect in somatic hypermutation have impaired gut homeostasis and compromised mucosal defense. *Nat. Immunol.* **12,** 264–270 (2011).

25. Wirtz, S., Neufert, C., Weigmann, B. & Neurath, M. F. Chemically induced mouse models of intestinal inflammation. *Nat. Protoc.* **2,** 541–546 (2007).

26. Mirpuri, J. *et al.* Proteobacteria-specific IgA regulates maturation of the intestinal microbiota. 1–12 (2014).

27. Palm, N. W. *et al.* Immunoglobulin A Coating Identifies Colitogenic Bacteria in Inflammatory Bowel Disease. *Cell* **158,** 1000–1010 (2014).

28. Hooper, L. V. Interactions Between the Microbiota and the Immune System. *Science* **336,** 1268 (2012).

29. Mowat, A. M. & Agace, W. W. Regional specialization within the intestinal immune system. *Nat. Rev. Immunol*. **14,** (2014).

30. Cash, H. L., Whitham, C. V, Behrendt, C. L. & Hooper, L. V. Symbiotic Bacteria Direct Expression of an Intestinal Bactericidal Lectin. *Science*. **313,** 1126–1130 (2009).

31. Vaishnava, S. *et al.* The Antibacterial Lectin RegIIIγ Promotes the Spatial Segregation of Microbiota and Host in the Intestine. *Science* **334,** 255 (2011).

32. Solnick, J. V. & Schauer, D. B. Emergence of Diverse *Helicobacter* Species in the Pathogenesis of Gastric and Entherohepatic Diseases. *Clinic. Microbiol. Rev* **14,** 59-97 (2001).
33. Suerbaum, S. *et al.* The complete genome sequence of the carcinogenic bacterium Helicobacter hepaticus. *Proc. Natl. Acad. Sci. U. S. A.* **100,** 7901–7906 (2003).

34. Wasimuddin *et al.* High Prevalence and Species Diversity of *Helicobacter* spp. Detected in Wild House Mice. *Appl. Environ. Microbiol* **78,** 8158-8160 (2012).

35. Kullberg M. C. *et al. Helicobacter hepaticus* triggers colitis in specific-pathogen free interleukin-10 (IL-10)-deficient mice through an IL-12- and gamma interferon-dependent mechanism. *Infect. Immun*. **66**, 5157-5166 (1998).

36. Whary, M. T. *et al.* Long-term Colonization Levels of *Helicobacter hepaticus* in the Cecum of Hepatitis-Prone A/JCr Mice Are Significantly Lower Than Those in Hepatitis-Resistant C57BL/6 Mice. *Comp. Med*. **51**, 413-417 (2001).

37. Zhang, L. *et al*. Natural colonization with Helicobacter species and the development of inflammatory bowel disease in interleukin-10-deficient mice. *Helicobacter.* **10,** 223-30 (2005).

38. Livingston, R. S. *et al.* Transmission of *Helicobacter hepaticus* infection to sentinel mice by contaminated bedding. *Lab. Anim. Sci*. **48**, 291-293 (1998).

39. Taylor, N. S., Xu, S., Nambiar, P., Dewhirst, F. E. & Fox, J. G. Enterohepatic *Helicobacter* species are prevalent in mice from commercial and academic institutions in Asia, Europe, and North America. *J. Clin. Microbiol.* **45,** 2166–2172 (2007).

40. Chichlowski, M. & Hale, L. P. Effects of *Helicobacter* infection on research: The case for eradication of *Helicobacter* from rodent research. *Comp. Med.* **59,** 10–17 (2009).

41. Chow, J., Tang, H., and Mazmanian, S., K. Pathobionts of the Gastrointestinal Microbiota and Inflammatory Disease. *Curr. Opin. Immunol*. **23**, 473–480 (2011).

42. Grenham, S., Clarke, G., Cryan, J. F., Dinan, T. G. Brain–Gut–Microbe Communication in Health and Disease. *Front Physiol*. 2: 94 (2011).

43. Petnicki-Ocwieja T., *et al.* Nod2 is required for the regulation of commensal microbiota in the intestine. Proc. Natl. Acad. Sci. **106,** 15813-15818 (2009).

44. Ihrig, M., Schrenzel, M. D., and Fox, J. G. Differential susceptibility to hepatic inflammation and proliferation in AXB recombinant inbred mice chronically infected with *Helicobacter hepaticus*.Am. J. Pathol. **155,** 571-582 (1999).
45. Truett, G. E. *et al.* Preparation of PCR-quality mouse genomic DNA with hot sodium hydroxide and tris (HotSHOT). *Biotech*. **29**, 52-54 (2000).

Websites
Figure 3. Mouse GI tract and visceral anatomy.

46. (A) Adapted from Cook, M. J. The Anatomy of the Laboratory Mouse. (1965). Retrieved from http://www.informatics.jax.org/cookbook/figures/figure57.shtml on September 27, 20:38h.

47. (B) Adapted from Revised Guides for Organ Sampling and Trimming in Rats and Mice. National Institute of Environmental Health Sciences (NIH). (2011). Retrieved from https://www.niehs.nih.gov/research/resources/visual-guides/guides/livers/index.cfm on September 27, 20:38h.

6. APPENDIX

6.1. Original approach of the project

From previous studies developed by our group, it was revealed that *Hh* colonization of healthy newborn B6 WT mice induced a tolerant response indicated by: the fact that animals did not mount a specific Ig response against these bacteria; exhibited high *Hh* faecal loads; maintenance of tolerance until adult life (unpublished data). Conversely, adult-colonization with *Hh* elicited a robust *Hh*-specific Ig response and a reduction of bacterial load (unpublished data).

In light of the evidences indicating a sustained tolerant state to *Hh* beyond maturation to adult, the aim of the initial project was to understand whether this tolerogenic response is the result of an exclusive co-evolved host- *Hh* mutualistic relationship, or whether it can be seen for different commensal bacteria.

Decomposing this question, besides exploring if this tolerogenic property is shared with other bacteria of the gut microbiota we also questioned whether the ability to generate tolerance in the host is promoted by *Hh*. To address this, we selected two distinct candidates: *Lactobacillus reuteri*, non-pathogenic/commensal, and *Pseudomonas aeruginosa*, an opportunistic pathogen. Our experimental approach comprised the quantification of faecal bacterial load and relative amount of specific-IgA produced against the two candidates, as it was done for *Hh* in our lab. Both candidates were tested in faecal and intestinal tissue DNA samples from B6 WT and Rag2-deficient ($Rag2^{-/-}$; lacking mature B and T lymphocytes) mice by PCR; using species-specific primers for each. In addition, we used primers restricted to *P. aeruginosa*. None of the candidates was detected in samples of DNA from intestinal tissue; nevertheless, we detected *L. reuteri* in faecal DNA from both genotypes (WT and $Rag2^{-/-}$). Presumably, we were not able to detect *P. aeruginosa* because it is not present in intestinal microbiota of conventional SPF (Specific-Pathogen-Free) mice from our facility.

Apart from these results, we decided to use a different strategy: detection of IgA-coated (IgA^{+}) faecal bacteria from non-colonized (SPF), adult- and newborn-colonized mice with *Hh* using a staining with an anti-IgA FITC antibody and a nucleic acid stain (Syto 9). Our subsequent approach included sorting of the IgA^{+} and IgA^{-} faecal bacteria populations (coated vs non-coated with IgA) from each experimental group. After bacterial sorting, we would identify the bacterial genera present in both IgA^{+} and IgA^{-} populations by 16S sequencing and evaluate the differences between SPF and *Hh*-colonized mice and between adult- and newborn-colonized mice. If *Hh* can favour tolerance to other bacteria, we would expect that IgA^{+} bacteria could become IgA^{-} in its presence.

This experimental approach became very ambitious for the time frame of the project and we faced several complications through its execution. Primarily, the anti-IgA FITC antibody used for flow cytometric analysis did not allow a reliable detection of IgA-coated bacteria; even after antibody titration and modifications in our stain protocol (stain volume, incubation time, number of washes with PBS, etc.) we were never able to attain an effective stain.
Alternatively, we decided to stain our samples with the goat anti-mouse IgA capture antibody used for the ELISA assay, labelling it for flow cytometric analysis. This anti-IgA revealed a consistent and robust staining of our samples (it was used for the incubation of faecal extract with cultured *Hh*, shown ahead in this work). However, on the days planned for sorting of the 2 IgA populations (which requires, at least, 10^6 events – several hours of sorting – for further DNA extraction and 16S sequencing analysis) the stain was not as efficient as before, leading to insufficient number of sorted events.

6.2. Growth of *Hh* in culture

Bacteria (*H. hepaticus* ATCC 51449 strain) grown in culture were provided by Margarida Parente (Molecular Genetics of Microbial Resistance, ITQB, Oeiras).

The strain was routinely cultivated on blood agar (BA) plates which are composed of solid medium Blood Agar Base nº2 (Oxoid) supplemented with 10% defibrinated horse blood (Probiológica) and an antibiotic-antifungal mix containing 6.3 g/L vancomycin (Roth), 3.1 g/L trimethroprim (Sigma) and 2.5 g/L amphotericin B (Roth). Cells were incubated in closed jars, at 37°C, under a microaerobic atmosphere (7% CO_2, 6% O_2, 3.5% H_2 and 83.5% N_2) generated by an Anoxomat system (Mart Microbiology). Bacteria were taken as fully grown when cultured in BA plates for 5 days, with two serial passages. After growth on BA plates for 5 days, bacterial colonies were scraped from the plates and suspended in PBS, into several dilutions. Bacterial density was estimated by measuring the OD (absorbance) 600 nm of the serially diluted bacterial suspensions, in order to obtain at least one plate with a countable number of bacteria (CFU). After counting the colonies (CFU) the matching between OD of each bacterial suspension and the number of colonies was done. Hence, in a bacterial suspension from which the OD 600 nm is 1, we have 1.5E10 CFU/ml bacteria.

6.3. Faecal extract serial dilution preparation

Table 6.3. 96 well plate representation of faecal extract serial dilution preparation.

Plate	Sample	1	2	3	4	5	6	
	Dilution	SPF1	SPF2	Ad.col1	Ad.col2	Nb.col1	Nb.col.2	**Dilution**
A	**1**	30 µl f.e.	30 µl f.e.	30 µl f.e.	30 µl f.e.	30 µl f.e.	30 µl f.e.	10 µl down
B	**3**	20 µl PBS	20 µl PBS	20 µl PBS	20 µl PBS	20 µl PBS	20 µl PBS	10 µl down
C	**9**	20 µl PBS	20 µl PBS	20 µl PBS	20 µl PBS	20 µl PBS	20 µl PBS	10 µl down
D	**27**	20 µl PBS	20 µl PBS	20 µl PBS	20 µl PBS	20 µl PBS	20 µl PBS	10 µl out

From each undiluted faecal extract sample, 10 µl were removed and homogenized in 20 µl of PBS, reducing serially into 1:3, 1:9 and 1:27 concentrations.

Incubation of faecal extracts with cultured *Hh* was performed on a plate, on ice, for 30 minutes. After incubation, the content from each well was transferred into 1.5 ml tubes for further incubation with both Goat Anti-Mouse IgA labelled with Alexa 647 (Ana Regalado, Antibody Service, Instituto Gulbenkian de Ciência; catalogue number 1040-01, Southern Biotech) and Syto9 nucleic acid stain (3.34 mM solution in DMSO; Live/Dead Bac Light^{TM} Bacterial Viability and counting kit, L34856 Lot 1099894, Molecular Probes, Invitrogen).

f.e. – faecal extract. The plate represented below, corresponds to one experiment. The results shown in section 3.3. (Results) were pooled from two independent experiments. SPF (n=3). Ad.col mice (n=5). Nb.col mice (n=5).

6.4. Primers used in this study

Table 6.4. Bacterial primer sets used for PCR and qPCR.

DNA target	Primer set	Product size (bp)	Reference
H. hepaticus 16S rRNA[1]	GCATTTGAAACTGTTACTCTG CTGTTTTCAAGCTCCCCGAAG	417	43
Eubacteria (Universal) 16S rRNA	ACTCCTACGGGAGGCAGCAGT ATTACCGCGGCTGCTGGC	~170	31
18S rRNA[2] (host DNA)	CATTCGAACGTCTGCCCTAT CCTGCTGCCTTCCTTGGA	137	31

[1] Specific for *H. hepaticus* 16S (confirmed by sequencing).

[2] Component of the small eukaryotic ribosomal subunit (normalizer for the intestinal/organ tissue DNA)

6.5. Mice used for *Hh* load analysis by qPCR within the gut and organs

Table 6.5. Conventional SPF experimentally colonized with *Hh* used for the study of *Hh* distribution throughout the GI tract and ability to colonize other internal organs. Mouse strain, genotypes and *Hh* colonization conditions from the animals analysed in sections 3.4. and 3.5. (Results).

# mice	Sex	Genotype	*Hh* colonization status
3*	M	C57BL/6 WT	Newborn-colonized
3*	F	C57BL/6 WT	Newborn-colonized
4	M	C57BL/6 WT	Adult-colonized
4	M	C57BL/6 Rag2$^{-/-}$	Adult-colonized
5	F	C57BL/6 WT	Adult-colonized
6	F	C57BL/6 WT	Newborn-colonized

***** Only collection of the different intestinal regions.

6.6. Standards used for qPCR analysis of *Hh* load

Table 6.6. Standard curve preparation for *Hh* load quantification by qPCR.

DNA target	Number of copies/ng	Standard points (ng/µl)
Segment amplified with *Hh* 16S rRNA-specific primers using pGEM-T Easy vector + 417, 1:1000	2.69E+08	2.00E+06 2.00E+04 2.00E+02 2.00E+01
Segment of the 16S rRNA gene amplified using Eubacteria – Universal – primers in *E. coli* DNA	1.40E+06	2.00E+07 2.00E+06 2.00E+04 2.00E+02
18S rRNA (host DNA)	*	18.28* 1.83* 0.18*

We used 2 µl of DNA template for each of the standard points in 8 µl of SyBR Green qPCR mix.

*For the 18S rRNA gene: we used 10 fold dilutions of DNA purified from intestinal tissue (SPF Rag2$^{-/-}$ mouse; concentration shown corresponds to 2 µl volume used in the qPCR)